A THESIS

FOR THE DEGREE OF DOCTOR OF PHILOSOPHY

Biological effects of *Pyropia yezoensis* and identification of their chemical structures

Ji-Hyeok Lee

Department of Aquatic Life Medicine

GRADUATE SCHOOL

JEJU NATIONAL UNIVERSITY

February, 2015

Biological effects of *Pyropia yezoensis* and identification of their chemical structures

Ji-Hyeok Lee

(Supervised by Professor You-Jin Jeon)

A thesis submitted in partial fulfillment of the requirement for the degree of

DOCTOR OF PHILOSOPHY

This thesis has been examined and approved by

_____

Thesis director, Seung-Heon Lee, Professor of Marine Life Science, Jeju National University

_____

Seung-Cheol Lee, Professor of Kyeong Sang national University

_____

Ki-Nam Kim, Researcher of Jeju Biodiversity Research Institute

_____

Chan-Won Han, Professor of College of Veterinary Medicine, Jeju National University

_____

You-Jin Jeon, Professor of Marine Life Science, Jeju National University

Date

Department of Marine Life Science

GRADUATE SCHOOL

JEJU NATIONAL UNIVERSITY

CONTENTS

국문초록

김은예로부터식품및의약재료로사용되어지고있으며, 항산화, 항염, 항고혈압등과같은생리활성이알려져왔다.

하지만이들에대한명확한생리활성에관한연구가진행되어진바가없어, 이연구에서는김의항염및항당뇨효능을평가하고유용성분을규명하였다.

항염의경우에는세균외독소인 lipopolysaccharide (LPS)에의해 RAW 264.7 세포내에유발되어진염증성매개체인, nitric oxide (NO) 및 PGE2, TNF-α, IL-1β, IL-6와염증성단백질인 iNOS와 COX-2에대한김의효능평가를수행하였으며, 또한 NF-κB와 MAPKs pathway 검증을통해이들의항염증메커니즘을규명하였다. 그리고김의간염및간섬유화에대한효능은자극물질인 ethanol과 CCl_4, 그리고 TAA를통해제작된 zebrafish 간염및간섬유화모델을적용하여평가하였다. 또한김의항당뇨평가를위하여, α-glucosidase저해효능과 zebrafish 혈액내 glucose 함량변화등을평가하였으며, 특히마우스유래근육세포인 C2C12내 glucose transfer인 Glut 4 transformation 유도단백질인 AMPK와

AKT의활성화측정을통하여김의항당뇨효능을평가하였다.

1. 방사무늬김유래추출물에서나온각 n-Hexane, $CHCl_3$, EtOAc, Water 분획물중 n-Hexane 분획물이가장높은항염증효능을보였으며, 이분획물로부터활성성분을분리하기위하여고속원심분배크로마토그래피를이용하였다. 분리된 compounds들중 PYH5과 PYH6가가장우수한 NO 생성저해효능을보였으며,이들은, 각각(11Z,13E,15E)-17-(5-hydroxycyclohexa-1,3-dienyl)heptadeca-11,13,15-trien-2-one와1-ethyl-3-(3-(3-methylbutan-2-yl)-14-phenyltetradecyl)benzene으로규명되어졌다.

2. PYH5은염증성매개체인 PGE_2, IL-1β, TNF-α를농도의존적으로감소시켰으며, 특히 NO와 PGE2를방출시키는염증성단백질인 iNOS와 COX-2에대한강력한생성저해효능을보였다. LPS에대한주요염증성매카니즘인 MAPK와 NF-κB pathways에대한평가결과, MAPK 단백질인 ERK1/2, p38, JNK중, ERK1/2를강력하게저해하였으며, 세포질내활성화된 NF-κB의생성을저해시켰다. PYH6 또한염증성매개체를농도의존적으로감소시켰으며, 염증성단백질인 iNOS와 COX-2를농도의존적으로감소시켰다. 하지만, MAPK와 NF-κB

128 pathway를경로하지않는것으로보아, 그외 AKT

129 pathway등의다른경로를통할것으로사료되어진다.

130 3. 김의 n-Hexane 분획물에서분리된화합물들중 PYH4가가장우수한α-glucosidase

131 저해효능을보였을뿐만아니라, 마우스근육세포인C2C12 세포내 glucose

132 uptake 효능이가장우수하였다. PYH4는 1H과 13C NMR 분석결과(E)-5-(8-

133 hydroxynon-6-enyl)cyclohexa-2,4-dienol으로규명되어졌다.

134 4. PYH4에대한*in vitro*와*in vivo*항당뇨평가결과, α-

135 glucosidase의저해효능은대조군인 Acarbose보다우수한 74 μg/ml (IC_{50}

136 value)의높은활성을보였으며, molecular Docker를통한α-glucosidase active

137 site에대한결합력을조사한결과, 강력한결합에너지를보였다. 특히, zebrafish

138 혈액내 glucose 함량을크게줄이는효능을보였으며, GLUT4

139 transformation의매개체인AMPK와 AKT의활성을크게증가시켰다.

140 결과적으로세포막내 $GLUT_4$를활성화시켜세포내로 glucose

141 흡입을유도시켰다.

142 5. 염증성질환중하나인, 간염과만성으로인한간섬유화에대한평가를하기위하여,

143 ethanol과 CCl_4에의한 zebrafish 간염및간섬유모델개발과 PYH5와

PYH6의간보호효능및항간염, 항간섬유화에대한평가결과, 1% ethanol 처리군은비처리군에비해매우높은간손상(GOP, GPT)을보였으며, 특히 PYH5와 PYH6 처리군은농도구배적으로간손상을낮추었다. 또한 1% ethanol을매일처리한군은염증성매개체인 IL-1β와 IL-6, TNF-α, iNOS를대폭증가시켰으며, 반면PYH5와 PYH6는염증성매개체들을 ethanol 처리군대비유의적으로낮춰주었다. 하지만, 1% ethanol의 4주간처리에의해간섬유화유도염증성매개체인 TGF-β1의경우유도되지않았다. 기존에잘알려진간염및간경화유도물질인 CCl_4는 1주일에2회투여시간손상병변을유도하였으며, 또한염증성매개체들을대폭증가시켰다.특히 CCl_4의경우에는 3주째처리군에서간섬유화유도염증매개체인 TGF-β1이강하게발현되었다.

결론적으로, 방사무늬김에는염증성질병에관한강력한성분인(11Z,13E,15E)-17-(5-hydroxycyclohexa-1,3-dienyl)heptadeca-11,13,15-trien-2-one와 1-ethyl-3-(3-(3-methylbutan-2-yl)-14-phenyltetradecyl)benzene 이존재하였으며, 특히, zebrafish는 ethanol 및 CCl_4에의해유도된간염및간섬유화모델로서매우적합하였다. 그리고, 우리는방사무늬김유래컴파운드인(E)-5-(8-hydroxynon-6-enyl)cyclohexa-2,4-

dienol은당뇨에매우강력한물질임을제안할수있다.

LIST OF FIGURES

Figure 1.Microwave assistant rapid enzyme digest system (A) and process schematicdiagram (B) for obtain of the polysaccharides fraction, high and low molecular weight polysaccharides from dried *P. yezoensis*.

Figure 2.Degree of hydrolyses (DH) of the microwave assistant hydrolysis, the enzymatic hydrolysis (2 h) and the microwave assistant enzymatic hydrolysis from *P. yezoensis*.The microwave assistantextract was prepared using only MAREDS (40 W and 2 h); the enzymatic hydrolysate was prepared with only AMG (ratio of substrate to enzyme = 10:1); the microwave assistant enzymatic hydrolysate was prepared with AMG in MAREDS (40 W and 2 h). Graph values were described with log. *Significantly different from microwave assistant ($P < 0.05$);**Significantly different from microwave assistant ($P < 0.01$). +Significantly different from the microwave assistant enzymatic hydrolysate at 10 min ($P < 0.05$); ++Significantly different from the microwave assistant enzymatic hydrolysate at 10 min ($P < 0.01$).

Figure 3. Chromatograms of monosaccharides in the unfractioned polysaccharides (A), AMG-HMWP (B) and AMG-LMWP(C) from *P. yezoensis* and their contents (D).* 1: Galactose, 2: Glucose, 3: Manose

Figure 4.NO inhibitory effects of the fractions from 70% EtOH of *P. yezoensis* in LPS-induced RAW 264.7 cells

LIST OF TABLES

Introduction

Pyropia species, the important edible red algae, are well known as food and medicine in East and Southeast Asia including Korea, Japan, Taiwan and China. Various continents have been conformed in Porphyra species, including sulfated polysaccharide, mycosporine like amino acids, sterols, carotenoids, protein, essential fatty acids, vitamins, and minerals (Kazlowska et al., 2013; Senevirathne et al., 2010).

Among various functional continents, porphyran, sulphated polysaccharide related to agarose which composed of alternating units of 1,4-linked 3,6-anhydro-$_{L}$-galactose and 1,3-linked-$_{D}$-galacose residues, is constituted $_{D}$-galactose, 3,6-anhydro-$_{L}$-galactose, 6-*O*-methyl-$_{D}$-galactose as the main cell wall component of red algae (Hatada et al., 2006; Jiang et al., 2012), and has been known to have a variety of physiological effects such as anti-oxidant, -cancer, -hyperlipidemic, -fatigue, improvement of immunology and hypercholesterolemic activities (She et al., 2005; Ren et al., 1994; Guo et al., 2005; Inoue et al., 2009). As another one, mycosporine-like amino acids (MAAs) are small, colorless and water-soluble compounds composed of a cyclohexenone or cyclohexenimine chromophore conjugated with the nitrogen subsituent of an amino acids or its imino alcohol (Nakamura et at., 1982; Carreto et al., 1990; Shailendra et al., 2008), and have been identified in a wide variety of marine organisoms including, fungi, heterotrophic bacteria, cyanobacteria, eykaryotic algae and fish (Sinha et al., 1999). And among various functional minor compounds such as β-carotene,

chlorophyll a, phenolic compounds, sterols, several amino acids and fatty acids are also existed in *Pyropia* sp., and especially, β-carotene from *Pyropia* sp. exhibited protective effect against mutagenesis probably associated with carcinogenesis and reactive oxygen species (ROSs) (Okai et al., 1996; Nakayama et la., 1999). Sterols, including cholesterol, β-sitosterol and campesterol showed potential for protecting an organism from 4T1 cell-vased tumor genesis (Kazlowska et al., 2013). And Kazlowska et al. (2012) reported phenolic compounds from *Porphyra dentate* suppressed NO production in lipopolysaccharide (LPS)-stimulated macrophages via NF-κB-dependent iNOS gene transcription. Therefore, existences of these functional continents in *Pyropia* sp. are very important factors for revelation of various biological effects. However, the amounts of these biological active continents are easily changed by environment factors such as UV and temperature (Priya et al., 2008; Shailendra et al., 2008), and, especially, systematic experiments on *Pyropia* sp. produced in different environments haven't been performed. Therefore, in this study, we demonstrated various approximate, functional continents and biological effects of *Pyropia* sp. collected from different three areas with Gunsan, Janheung and Kwangcheon in S. Korea.

Inflammation represents a highly coordinated set of events that allow the tissues to respond against an injury or infection. It involves the participation of various cell-types expressing and reacting to the diverse mediators along a very precise sequence of events (Babu *et al*., 2009). Usually, inflammation is initiated through the production of specific cytokines or chemokines characterized by the recruitment of leukocytes to the damage sites. However, the sustained or excessive inflammation can lead to various diseases including rheumatoid arthritis, psoriasis and inflammatory bowel disease (Simon and Green, 2005). Macrophages play a key role in the inflammatory and immune reactions by releasing a

variety of inflammatory mediators such as nitric oxide (NO), tumor necrosis factor-α (TNF-α), interleukin-1 β (IL-1β), inducible nitric oxide synthase (iNOS) and cyclooxygenase-2 (COX-2) (Yoon et al., 2003; Ramana and Srivastava.,2006; Nunez Miguel et al., 2007). Lipopolysaccharide (LPS), a component of the gram negative cell wall, was used to stimulate peritoneal macrophages and induce the production of anti-inflammatory cytokines in the infection response (Pan et al., 2008). Initial features are of nonspecific flu-like symptoms, common to almost all acute viral infections and may include malaise, muscle and joint aches, fever, nausea or vomiting, diarrhea, and headache. More specific symptoms, which can be present in acute hepatitis from any cause, are: profound loss of appetite, aversion to smoking among smokers, dark urine, yellowing of the eyes and skin, and abdominal discomfort. Physical findings are usually minimal, apart from yellowing of the skin and conjunctivae, tender enlargement of the liver, enlarged lymph nodes in 5%, and enlargement of the spleen. Chronic hepatitis may cause nonspecific symptoms such as malaise, tiredness and weakness, and often leads to no symptoms at all. It is commonly identified on blood tests performed either for screening or to evaluate nonspecific symptoms. The presence of jaundice indicates advanced liver damage.

Liver inflammation is a reaction that occurs when liver cells are attacked by a disease-causing microbe or substance. The liver is an organ in the digestive system that assists the digestive process and carries out many other essential functions. These functions include producing bile to help break down food into energy; creating essential substances, such as hormones; cleaning toxins from the blood, including those from medication, alcohol and drugs; and controlling fat storage and cholesterol production and release.

Alcoholic liver disease is a term that encompasses the hepatic manifestations of alcohol

316 overconsumption, including fatty liver, alcoholic hepatitis, and chronic hepatitis with hepatic
317 fibrosis or cirrhosis (O'Shea et al., 2010). It is the major cause of liver disease in Western
318 countries. Although steatosis (fatty liver) will develop in any individual who consumes a
319 large quantity of alcoholic beverages over a long period of time, this process is transient and
320 reversible (O'Shea et al., 2010). Of all chronic heavy drinkers, only 15–20% develop hepatitis
321 or cirrhosis, which can occur concomitantly or in succession (Menon et al., 2001). How
322 alcohol damages the liver is not completely understood. 80% of alcohol passes through the
323 liver to be detoxified. Chronic consumption of alcohol results in the secretion of pro-
324 inflammatory cytokines (TNF-alpha, Interleukin 6 [IL-6] and Interleukin 8 [IL-8]), oxidative
325 stress, lipid peroxidation, and acetaldehyde toxicity. These factors cause inflammation,
326 apoptosis and eventually fibrosis of liver cells. Why this occurs in only a few individuals is
327 still unclear. Additionally, the liver has tremendous capacity to regenerate and even when
328 75% of hepatocytes are dead, it continues to function as normal (Longstreth & Zieve, 2009).

329 Fibrosis is the formation of excess fibrous connective tissue in an organ or tissue in a
330 reparative or reactive process (Birbrair et. al., 2013). This can be a reactive, benign, or
331 pathological state. In response to injury this is called scarring and if fibrosis arises from a
332 single cell line this is called a fibroma. Physiologically this acts to deposit connective tissue,
333 which can obliterate the architecture and function of the underlying organ or tissue. Fibrosis
334 can be used to describe the pathological state of excess deposition of fibrous tissue, as well as
335 the process of connective tissue deposition in healing (DermNet NZ). Fibrosis is similar to
336 the process of scarring, in that both involve stimulated cells laying down connective tissue,
337 including collagen and glycosaminoglycans. Immune cells called Macrophages, and damaged
338 tissue between surfaces called interstitium release TGF beta. This can be because of

numerous reasons, including inflammation of the nearby tissue, or a generalised inflammatory state, with increased circulating mediators. TGF beta stimulates the proliferation and activation of fibroblasts, which deposit connective tissue (Trojanowska, 2012).

Cirrhosis is a late stage of serious liver disease marked by inflammation (swelling), fibrosis (cellular hardening) and damaged membranes preventing detoxification of chemicals in the body, ending in scarring and necrosis (cell death). Between 10% to 20% of heavy drinkers will develop cirrhosis of the liver (NIAAA, 1993). Acetaldehyde may be responsible for alcohol-induced fibrosis by stimulating collagen deposition by hepatic stellate cells (Menon et al., 2001). The production of oxidants derived from NADPH oxi- dase and/or cytochrome P-450 2E1 and the formation of acetaldehyde-protein adducts damage the cell membrane (Menon et al., 2001). Symptoms include jaundice (yellowing), liver enlargement, and pain and tenderness from the structural changes in damaged liver architecture. Without total abstinence from alcohol use, will eventually lead to liver failure. Late complications of cirrhosis or liver failure include portal hypertension (high blood pressure in the portal vein due to the increased flow resistance through the damaged liver), coagulation disorders (due to impaired production of coagulation factors), ascites (heavy abdominal swelling due to buildup of fluids in the tissues) and other complications, including hepatic encephalopathy and the hepatorenal syndrome. Cirrhosis can also result from other causes than alcohol abuse, such as viral hepatitis and heavy exposure to toxins other than alcohol. The late stages of cirrhosis may look similar medically, regardless of cause. This phenomenon is termed the "final common pathway" for the disease. Fatty change and alcoholic hepatitis with abstinence can be reversible. The later stages of fibrosis and cirrhosis tend to be irreversible, but can

362 usually be contained with abstinence for long periods of time.

363 The zebrafish (Danio rerio) is a tropical freshwater fish belonging to the minnow family
364 (Cyprinidae) of the order Cypriniformes (Froese et al., 2007). Native to the Himalayan region,
365 it is a popular aquarium fish, frequently sold under the trade name zebra danio. The zebrafish
366 is also an important vertebrate model organism in scientific research. It is particularly notable
367 for its regenerative abilities (Goldshmit et al., 2012) and has been modified by researchers to
368 produce several transgenic strains (White et al., 2008). Especially, zebrafish has severally
369 been introduced as cirrhosis model, but most of studies focus on the embryos and transgenic
370 strains. Recently, zebrafish has been used for various biological evaluations such as
371 antioxidant and anti-inflammation as alterative mouse and monkey models. But cirrhosis
372 model of zebrafish has been restrictively development, therefore we focused on development
373 of the liver inflammation and fibermodels of ethanol and CCl_4 stimulated adult zebrafish.
374 And anti-inflammatory active compounds from *P. yezoensis* was evaluated against liver
375 inflammation and fiber generated in ethanol-stimulated zebrafish.

376 Diabetes mellitus (DM), commonly referred to as diabetes, is a group of metabolic diseases
377 in which there are high blood sugar levels over a prolonged period. Symptoms of high blood
378 sugar include frequent urination, increased thirst, and increased hunger. If left untreated,
379 diabetes can cause many complications. Acute complications include diabetic ketoacidosis
380 and nonketotic hyperosmolar coma (Kitabchi et al., 2009) Serious long-term complications
381 include cardiovascular disease, stroke, kidney failure, foot ulcers and damage to the eyes.
382 Diabetes mellitus is classified into four broad categories: type 1, type 2, gestational diabetes,
383 and "other specific types" (David G. Gardner, 2011). Type 1 diabetes mellitus is
384 characterized by loss of the insulin-producing beta cells of the islets of Langerhans in the

pancreas, leading to insulin deficiency.Type 2 diabetes mellitus is characterized by insulin resistance, which may be combined with relatively reduced insulin secretion (David G. Gardner, 2011). Previous study, sulfated polysaccharide from *Pyropia* sp. has been reported an anti-diabetes effect, but there are various continents such as sterol, pigments, and polar compounds in red algae. Therefore we focused on identification of anti-diabetes compounds from *P. yezoensis* and performed the evaluation of *in vivo*, zebrafish model for diabetes.

Part-I

Identification of active compounds of *Pyropia yezoensis* on anti-inflammation

Abstract

This study focuses on a simply preparation of functional polysaccharides from *Pyropia yezoensis*, a marine red alga in a microwave assistant rapid enzyme digest system (MAREDS) with the carbohydrases, including Viscozyme, Celluclast, amyloglucosidase (AMG), Temamyl and Ultraflo, as well as evaluation of their antioxidative effect. Polysaccharide hydrolysates were manufactured in MAREDS under conditions with 40 W and different hydrolyzing times, and each hydrolytic condition (pH and temperature) of the carbohydrases. And then, polysaccharides of below and above 10 kDa were efficiently prepared using an ultrafilteration membrane of 10 kDa molecular weight cut-off. In the result, we confirmed that MAREDS helps to increase activation of AMG through the increased degree of hydrolysis, thus the best AMG assistant hydrolysate was manufactured with 10:1 (ratio of substrate to enzyme) for 2 h, occupied the highest degree of hydrolysis (25.02 %). And AMG hydrolysate showed to time-dependently increase the antioxidative effect. Especially, the low molecular weight polysaccharides (LMWP, < 10 kDa) from AMG

hydrolysate possessed higher antioxidant effect compared with the unfractionated polysaccharides and the high molecular weight polysaccharides (HMWPs, > 10 kDa), and was consisted of monosaccharides with galactose (27.25%), glucose (64.50%), and manose (8.23%), etc. which are different with the unfractionated polysaccharide and HMWP. Consequently, we could efficiently, simply and rapidly prepare the functional LMWP using both the MAREDS with the carbohydrase and ultrafilteration, and suggest that LMWP from *P. yezoensis* might be a valuable algal polysaccharide antioxidative agent.

Keywords: *Pyropia yezoensis*; microwave assistant rapid enzyme digest system; low molecular weight polysaccharides; antioxidative effect

1. Introduction

Pyropiayezoensis, is well known important edible red alga as food and medicine in Southeast Asia including Korea, Japan, Taiwan and China. There are various components, containing sulfated polysaccharides, mycosporine like amino acids, sterols, carotenoids, proteins, essential fatty acids, vitamins, and minerals in *P. yezoensis*.[1,2]

Among various functional components from *P. yezoensis*, polysaccharides have been used in food industry for a long time, because they have a variety of physiological effects such as anti-oxidant, -cancer, -hyperlipidemic and -fatigue as well as immunomodulatory and hypercholesterolemic activities.[3-6] Thus, many properties of polysaccharides depend on their molecular weights.[7] A molecular weight of polysaccharide is an important factor which is having relationship with biological effects. Especially, relatively lower molecular polysaccharides have been reported to have higher antioxidant and hepatoprotective effects

than higher molecular polysaccharides.[8,9]

Microwaves are composed of electric and magnetic fields, electromagnetic energy, and its spectral frequency range occupied from 300 to 300,000 MHz.[10,11] Microwave energy acts as a nonionizing radiation that causes rotation of the dipoles, and especially induces fragmentation of polymer structure and molecular weight of polysaccharides during microwave heating process.[11] Thus microwave irradiation has been applied to accelerate chemical or enzymatic reactions for proteomics applications.[12] Consequently, the microwave process is considered as useful for enzymatic hydrolysis of polysaccharide.

In this study, we demonstrate the preparation of the functional polysaccharides from *P. yezoensis* by microwave assistant rapid enzyme digest system (MAREDS) which offers solution for easy, fast and safe enzyme reactions with microwave (**Fig. 1(A)**) and and their antioxidant effect.

2. Materials and methods

2. 1. Materials

Pyropiayezoensis which was cultivated at the coast of Wando Island in South Korea, was washed twice with freshwater, and then immediately frozen and stored at –20℃ until use. The frozen samples were lyophilized and ground with a grinder. The dried sample powder was stored in refrigerator until use.

2. 2. Chemicals and reagents

2,2-azobis-(2-amidinopropane) dihydrochloride (AAPH) were purchased from Sigma Chemical Co. (USA). Caborhydrate hydrolytic enzymes such as Viscozyme, Ultraflo,

amyloglucosidase (AMG), Termarmyl and Celluclast were purchased from Novozyme Co. (Denmark). All the other chemicals used were of analytical grade.

2. 3. Approximate composition

The approximate composition of dried sample powders was determined according to the AOAC methods.[13] Moisture content was determined in a dry oven at 105℃ for 24 h, crude ash content by calcinations in furnace at 550℃, crude protein content by Kjeldahl method (Kjeltec^{TM}2300, Foss Co. Ltd., Denmark), and crude lipid content by Sohxlet method (Sohxlet system 1046, TacatorAB, Sweden).

2. 4. Preparation of polysaccharide fraction from dried *P. yezoensis*

For preparation of the polysaccharides fraction with high purity, we used to combine and modify the protocols reported by Cian et al. (2012) and Takahashi et al. (2000) (**Fig. 1(B)**). First, we could remove the water soluble proteins by distilled water (DW) at 20℃ from dried sample of 50 g, and then tried to remove a lipid fraction by 90% EtOH in 100℃ for 2 h. Finally, a 2 g of polysaccharides fraction was obtained 3 times from the residue by DW in 120℃ for 15 min after the step which removed the lipid.

2. 5. Hydrolysis of the crude polysaccharide fraction

Polysaccharides were hydrolyzed by MAREDS (REDS^{TM}, ASTA INC., USA) (**Fig. 1 (A)**) under the various conditions with the five enzymes including Viscozyme, Celluclast, Termamyl, AMG and Ultraflo, and their ratios of substrate to enzyme (10:1 and 100:1, respectively). The low molecular weight polysaccharides (LMWP) of below 10 kDa and the

499 high molecular weight polysaccaides (HMWP) of above 10 kDa were obtained through
500 AccuPrep® plastmid extraction kit equipped with 10 kDa molecular weight cut-off (MWCO)
501 ultrafilteration membrane (BIONEER, USA).
502

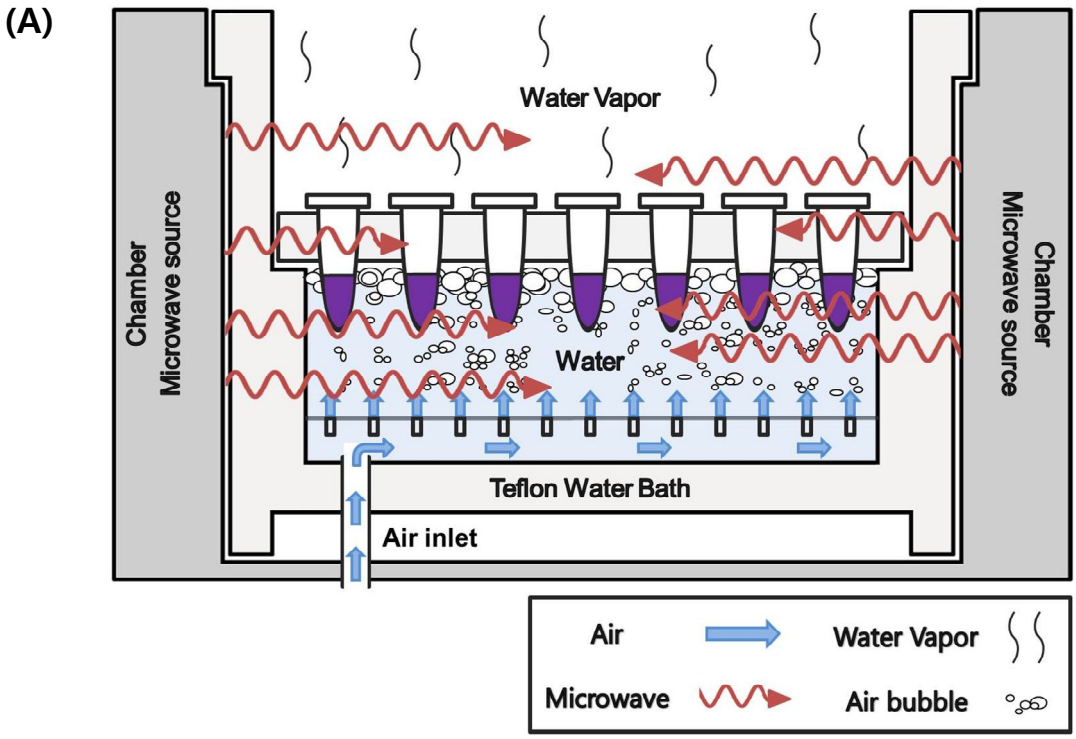

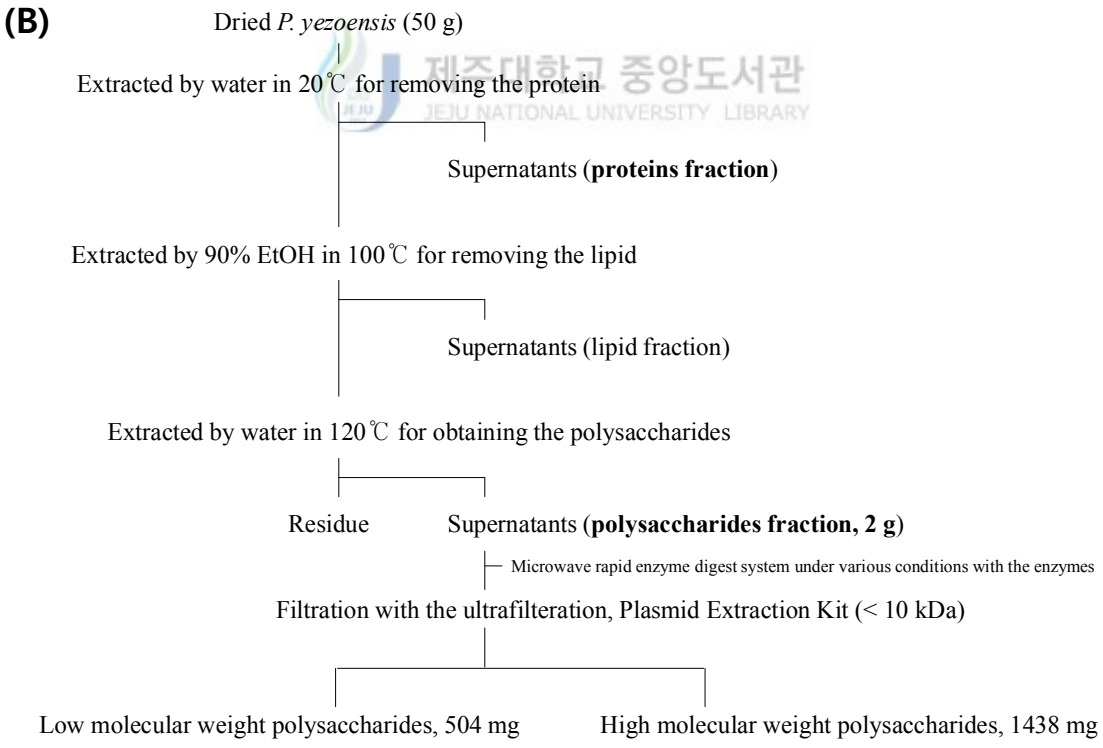

Fig. 1. Microwave assistant rapid enzyme digest system (A) and process schematicdiagram (B) for obtain of the polysaccharides fraction, high and low molecular weight

polysaccharides from dried *P. yezoensis*.

2. 6. Degree of hydrolysis (DH)

The sugar content was determined using phenol-sulfuric acid colorimetric method.[16] The DHs (%) of the polysaccharides from the enzymatic hydrolysates were calculated under the base on the total sugar contents in the LMWP after filtration of hydrolyzed polysaccharides fraction to the total sugar weight of crude polysaccharides fraction from *P. yezoensis* and its formulation indicated in below:

$$\text{DH (\%)} = \frac{\text{Total sugar contents (mg) of below 10 kDa}}{\text{Total sugar contents (mg) in the crude polysaccharides}} \times 100$$

2. 7. Antioxidative evaluation of polysaccharides

Alkyl radical scavenging activity was measured using the method described by Hiramoto et al. (1993). The experimental conditions of ESR (electron spin resonance) spectrometer (JES-FA machine, JEOL, Tokyo, Japan) were as followed; for alkyl, magnetic field 336.5±5 mT, power 1 mW, modulation frequency 100 kHz, amplitude 1×1000, modulation width 0.2 mT, sweep width 10 mT, sweep time 30 sec, time constant 0.03 sec. Hydrogen peroxide scavenging activity was determined according to the method of Heo et al. (2005). A hundred μl of 0.1 M phosphate buffer (pH 5.0) and the sample solution were mixed in a 96 microwell plate. A 20 μl of hydrogen peroxide was added to the mixture, and then incubated at 37℃ for 5 min. After the incubation, 30 μl of 1.25 mM ABTS and 30 μl of peroxidase (1 unit/ml) were added to the mixture, and then incubated at 37℃ for 10 min. The absorbance was read with an ELISA reader at 405 nm.

2. 8. Statistical analysis

All the measurements were made in triplicate and all values were represented as means ±

552 standard error. The results were subjected to an analysis of the variance (ANOVA) using the
553 Turkey test to analyze the difference. A value of $p < 0.05$ was considered to indicate
554 statistical significance.
555
556 **3. Results & discussion**
557 **3. 1. Proximate composition**
558 **Table 1** showed proximate composition of the dried *P. yezeonsis*. Polysaccharides were the
559 most abundant content in dried sample (44.6±2.3%), and proteins occupied the second
560 highest amount. The value of utilization of the proteins and carbohydrates is considered to be
561 very high, because red seaweeds such as *Pyropia* sp. have high levels of proteins and
562 fibers.[19,20] And the component analysis of crude proteins and polysaccharides obtained from
563 *P. yezoensis* using the step which described in **Fig 1 (B)** was shown in **Table 2**. The
564 polysaccharide fraction contained high sugar content with 91.71±5.07%, whereas low sulfate
565 content of 5.41%. Porphyran, sulfated polysaccharide, is a main component in *Pyropia* sp.,
566 and was reported to contain the sulfate content of about 8% in *P. yezoensis* similar with our
567 crude polysaccharides fraction.[15,21]
568
569
570
571
572
573
574

Table 1. Proximate composition of dried *P. yezoensis*

	Protein (%)	Carbohydrates (%)	Lipid (%)	Moisture (%)	Ash (%)	Calories (kcal/100g)
P. yezoensis	41.7±1.7	44.6±2.3	1.8±0.12	7.4±1.7	5.3±0.1	351.4±12.7

596

597

598

599

600

601

602

603

604 **Table 2.Crude polysaccharides, crude protein and sulfate content in the proteins and the**

605 **polysaccharides fraction from *P. yezoensis***

	Sugar (%)	Protein (%)	Sulfate (%)
Proteins fraction	11.2±0.43	89.03±7.35	-
Polysaccharides fraction	91.71±5.07	8.7±3.3	5.41±0.02

606

607

608

609

610

611

612

613 **3. 2. Degree of hydrolysis (DH) and antioxidant effects of polysaccharides**

614 **hydrolysates in MAREDS**

615 **Table 3** showed the DH of the polysaccharides hydrolysates prepared under various
616 hydrolytic conditions, including the different ratios of substrate to enzymes (10:1 and 100:1)
617 and the hydrolysis times (10 min, 30 min, 1 h, 2 h, 3 h and 4 h, respectively) in MAREDS
618 with 40 W. The DH of AMG hydrolysis was increased with the time of hydrolysis (10 min ~
619 4 h), whereas other enzymes didn't affect to the hydrolysis of the polysaccharides. And AMG
620 hydrolysis in MAREDS showed higher DH than AMG hydrolysis only and microwave
621 assistant only (**Fig. 2**). Thus, AMG hydrolysates in MAREDS approached the optimal
622 hydrolysis at 2 h, since then, no significant increase in DH. This result suggests that AMG
623 accelerated the hydrolyses of the polysaccharides in MAREDS within a short time of 2 h. In
624 previous reports, microwave assistant system has been utilized for not only improving
625 activities of proteases, but also applying to degradation and extraction of polysaccharides.[22-25]
626 Tsubaki et al. (2013) demonstrated that microwave energy with polyoxometalate clusters
627 promoted the hydrolyses of corn starch and crystalline cellulose. And, we understand with
628 these results that the microwave assistant system is a useful tool to accelerate the activation
629 of the carbohydrase. Besides AMG hydrolysate exhibited strong antioxidative effects against
630 alkyl radical and H_2O_2 in a dose dependent manner (**Table 4**). And, antioxidant effect was
631 increased with the time of digestion of AMG. Nomura et al. (1998) previously reported that
632 polysaccharides from *P. yezoensis* hydrolyzed by β-agarase stimulated macrophage
633 proliferation. Therefore, preparation of polysaccharides from *P. yezoensis* by enzymatic
634 hydrolyses enhances their functionalities. Finally, we selected AMG hydrolysate in
635 MAREDS at 2 h for the further experiments.
636
637

Table 3.Degree of hydrolysis (DH) of the polysaccharides hydrolysates from *P. yezoensis* in MAREDS

	Degree of hydrolysis (%)									
	Viscozyme		Celluclast		AMG		Termamyl		Ultraflo	
	10:1	100:1	10:1	100:1	10:1	100:1	10:1	100:1	10:1	100:1
10 min	12.11	0.65	4.51	1.51	8.65	6.42	4.90	5.37	2.84	2.90
30 min	14.78	2.98	3.55	1.01	15.78	7.73	3.54	5.86	3.83	3.59
1 h	13.57	2.70	6.56	1.16	13.96	7.66	2.32	5.07	2.97	2.17
2 h	13.05	1.59	5.73	1.16	25.02	9.00	5.30	4.80	3.19	0.98

Table 4. IC_{50} values on antioxidant effect of AMG hydrolysates in MAREDS

	IC_{50} values (mg/ml)	
	Alkyl radical	**H_2O_2**
AMG 10 min（10：1）	0.542±0.002	> 0.180
AMG 30 min（10：1）	0.482±0.018	0.175±0.000
AMG 1 h（10：1）	0.341±0.008	0.125±0.002
AMG 2 h（10：1）	0.196±0.001	0.096±0.002

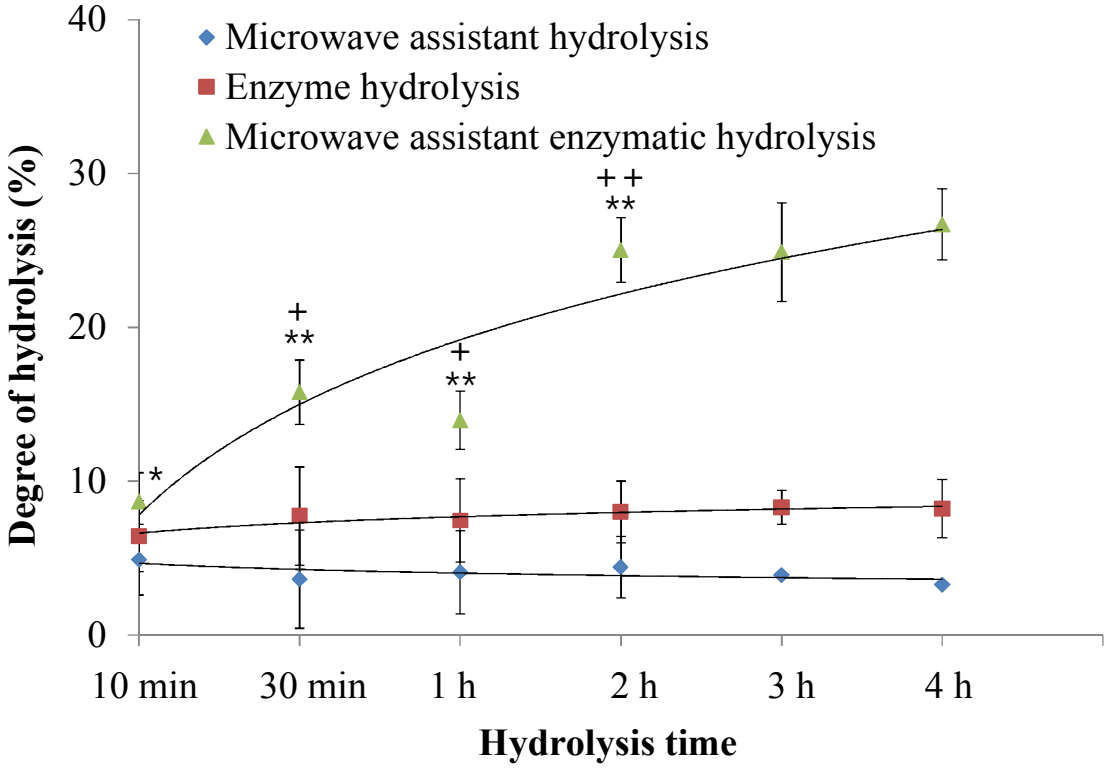

673

674 **Fig. 2.**Degree of hydrolyses (DH) of the microwave assistant hydrolysis, the enzymatic
675 hydrolysis (2 h) and the microwave assistant enzymatic hydrolysis from *P. yezoensis*.The
676 microwave assistantextract was prepared using only MAREDS (40 W and 2 h); the enzymatic
677 hydrolysate was prepared with only AMG (ratio of substrate to enzyme = 10:1); the
678 microwave assistant enzymatic hydrolysate was prepared with AMG in MAREDS (40 W and
679 2 h). Graph values were described with log. *Significantly different from microwave assistant
680 ($P < 0.05$);**Significantly different from microwave assistant ($P < 0.01$). +Significantly
681 different from the microwave assistant enzymatic hydrolysate at 10 min ($P < 0.05$);
682 ++Significantly different from the microwave assistant enzymatic hydrolysate at 10 min ($P <$
683 0.01).

684

685 **3. 3. Comparison of antioxidant effects between low and high molecular weight**

686 **polysaccharides from AMG hydrolysate**

687 The low and high molecular weight polysaccharides separated from AMG hydrolysate
688 (AMG-LMWP and AMG-HMWP, respectively) were prepared through the ultrafilteration of
689 10 kDa MWCO. AMG-LMWP exhibited stronger antioxidative effects against alkyl radical
690 and H_2O_2 than AMG-HMWP as well as the unfractioned AMG hydrolysate (**Table 4 and 5**).
691 This result suggests that molecular weights of the polysaccharides are quietly related to
692 antioxidant effect. Although biological effects with lower molecular weight polysaccharides
693 from *P. yezoensis* haven't been evaluated so far, some reports demonstrated that low
694 molecular weight polysaccharides and degraded polysaccharide from marine algal
695 polysaccharide showed higher antioxidant effects than high molecular weight
696 polysaccharides.[8,9]

697

698 **3. 4. Monosaccharide analysis of the polysaccharides from *P. yezoensis***

699 The monosaccharide compositions of AMG hydrolysate in MAREDS, AMG-HMWP and
700 AMG-LMWP were shown in **Fig. 3**. AMG-LMWP was consisted as monosaccharides with
701 galactose (27.25%), glucose (64.50%), and manose (8.25%) etc. Thus, the unfractioned
702 polysaccharides and AMG-HMWP showed higher galactose contents than AMG-LMWP
703 (93.60 and 92.28, respectively), whereas AMG-LMWP higher glucose content of 64.50%.
704 Also, AMG-LMWP contained lower sulfate content below 1%, compared to the
705 polysaccharide fraction (5.41%). Microwave generates the desulfation of sulfated
706 polysaccharides, without compromising seriously the molecular weight.[28]
707 Porphyran, sulphated polysaccharide related to agarose which composed of alternating units
708 of 1,4-linked 3,6-anhydro-$_L$-galactose and 1,3-linked-$_D$-galacose residues, is constituted $_D$-

galactose, 3,6-anhydro-$_L$-galactose, 6-*O*-methyl-$_D$-galactose as the main cell wall component of red algae,[29,30] and has been known to have a variety of physiological effects such as anti-oxidant, -cancer, -hyperlipidemic, -fatigue, improvement of immunology and hypercholesterolemic activities due to presence of sulfate.[4-6] However, in this study, the desulfated polysaccharide showed a remarkable enhanced antioxidant effect. This was considered that the biological effect was affected by the degradation and monosaccharides composition of polysaccharide during the microwave assistant enzymatic hydrolyzes. AMG hydrolyses 1,4- and 1,6-alpha linkages in liquefied starch. During the hydrolysis, glucose units are removed in a stepwise manner from the non-reducing end of the substrate molecule. The rate of hydrolysis depends upon the type of linkage as well as the chain length, i.e., 1,4-alpha linkages are hydrolysed more readily than 1,6-alpha linkages, and maltotriose and maltose are broken down at a lesser rate than longer chain oligosaccharides.[31] Therefore we suggest that AMG would hydrolyze the polysaccharide to break the 1,4-linked 3,6-anhydro-$_L$-galactose of the polysaccharide in *P. yezoensis*.

4. Conclusion

We could efficiently, simply and rapidly prepare AMG-LMWP by using both MAREDS and ultrafilteration, and AMG-LMWP might be a suitable candidate for an algal polysaccharide antioxidative agent.

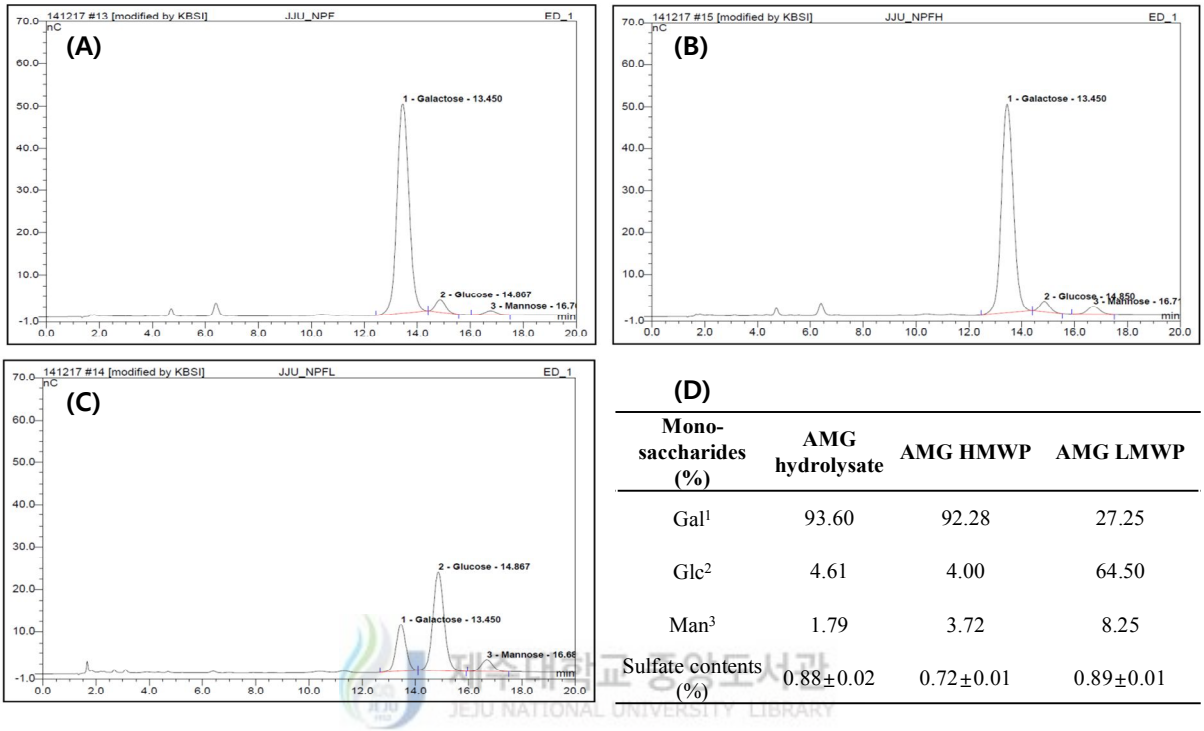

(D)

Mono-saccharides (%)	AMG hydrolysate	AMG HMWP	AMG LMWP
Gal[1]	93.60	92.28	27.25
Glc[2]	4.61	4.00	64.50
Man[3]	1.79	3.72	8.25
Sulfate contents (%)	0.88±0.02	0.72±0.01	0.89±0.01

Fig. 3. Chromatograms of monosaccharides in the unfractioned polysaccharides (A), AMG-HMWP (B) and AMG-LMWP(C) from *P. yezoensis* and their contents (D).* 1: Galactose, 2: Glucose, 3: Manose

Table 5. IC_{50} values on antioxidant effect of AMG-HMWP and LMWP in MAREDS

	IC_{50} values (μg/ml)	
	Alkyl radical	**H_2O_2**
AMG-HMWP (2 h, 10 : 1)	181.38±0.328	81±0.150
AMG-LMWPs (2 h ; 10 : 1)	114.36±3.476	13±0.000

Part-II

Anti-inflammatory compounds from *Pyropia yezoensis*, a marine red alga regulates the MAPK and NF- κB pathways

Abstract

This study was focus on isolation of anti-inflammatory compounds from *Pyropia yezoensis*, a marine red alga and identification of their anti-inflammatory effect via NF-κB and MAPK pathways. The 4 fractions with n-hexane (PYH), chloroform ($CHCl_3$, PYC), ethyl acetate (EtOAc, PYE) and water fractions (PYW) were prepared from 70 EtOH extract of *P. yezoensis*. Among them, PYH showed the strongest inhibitory activity against nitric oxide (NO) generated from lipopolysaccharide (LPS) stimulated RAW 264.7 macrophages without the cytotoxicity. The eight fractions (PYH1, PYH2-1~3, PYH3~6) were prepared from PYH by preparative centrifugal partition chromartography (CPC) with solvent condition consisted with n-hexane:EtOAc:methanol(MeOH):water (9:1:9:1). PYH5 and 6 exhibited higher anti-inflammatory effects on LPS-induced RAW 264.7 cells than others. Therefore, we identified chemical structures of PYH5 and PYH6 using NMR and LC-ESI/MS and they were confirmed as (11Z,13E,15E)-17-(5-hydroxycyclohexa-1,3-dienyl)heptadeca-11,13,15-trien-2-one (HTO) and 1-ethyl-3-(3-(3-methylbutan-2-yl)-14-phenyltetradecyl)benzene (EB), respectively. HTO and EB decreased the pro-inflammatory cytokines including TNF-α, IL-1β, and reduced production of PGE_2 released from COX-2. Thus, the protein expressions of COX-2 and iNOS which released nitric oxide (NO) and PGE2, respectively, were significantly increased by HTO and EB. Especially HTO exhibited anti-inflammatory effect

through decrease of NF-κB and MAPK protein, $ERK_{1/2}$ whereas EB only decreased the expression of MAPK proteins including p38, $ERK_{1/2}$. Consequently, we suggested that HTO regulates the MAPK and NF-κB pathways and EB relates with the MAPK pathway.

1. Materials and methods

2. 1. Materials

P. yezoensis was purchasedat Wondo, South Korea in February 2013, was ground and shifted through a 50 mesh standard testing sieve after dried by freeze dryer, and then the dried *P. yezoensis* was stored in refrigerator until use. All solvents used for preparation of crude sample and centrifugal partition chromatography (CPC) separation were of analytical grade (Daejung Chemicals &Metals Co., Seoul, Korea). High performance liquid chromatography (HPLC) grade solvents were purchased from Burdick & Jackson (MI, USA). Lipopolysaccharide (LPS) was purchased from sigma chemical Co., Ltd (ST. Louis, MO). Dulbecco's modified Eagle's medium (DMEM), fetal bovine serum (FBS) penicillin-strptomycin and trypsine-EDTA were obtained from Gibco/BRL (Grand Island, NY, USA). 3-(4,5-Dimethylthiazol-2-yl)-2,5-diphenyltetrazolium, dimethyl sulfoxide (DMSO) were purchased from Sigma (St. Louis, MO, USA). Other all reagents and solvents were purchased from Sigma (St. Louis, MO, USA).

2. 2. Apparatus

LLB-M high performance CPC (Sanki Engineering, Kyoto, Japan) was used as preparative CPC. The total cell volume is 240 mL. A four-way switching valve incorporated in the CPC apparatus allows operating in either the descending or the ascending mode. This

CPC system was equipped with a Hitachi 6000 pump (Hitachi, Japan), an L-4000 UV detector (Hitachi), and a Gilson FC 203B fraction collector (Gilson, France). The samples were manually injected through a Rheodyne valve (Rheodyne, CA, USA) with a 2 mL sample loop.

^{1}H-NMR spectra were measured with a JEOL JNM-LA 300 spectrometer and ^{13}C-NMR spectra with a Bruker AVANCE 400 spectrometer. Mass spectra (FAB-MS and EIMS) were recorded on a JEOL JMS 700 spectrometer.

2. 3. Preparation of crude extracts from *S. siliquastrum*

Dried *P. yezoensis*(60 g) was extracted three times for 24h with 70% EtOH at room temperature. The extract, concentrated in a rotary vacuum evaporator, partitioned with n-hexane, chloroform (CHCl3), ethyl acetate (EtOAc) and water, respectivley, and then the concentrated the fractions was stored in a refrigerator for CPC separation.

2. 4. CPC separation procedure

The CPC experiments were performed using a two-phase solvent system composed of *n*-hexane:ethyl acetate (EtOAc):methanol (MeOH):water (9:1:9:1, v/v). The two phases were separated after thoroughly equilibrating the mixture in a separating funnel at room temperature. The upper organic phase was used as the stationary phase, whereas the lower aqueous phase was employed as the mobile phase. The CPC column was initially filled with the organic stationary phase and then rotated at 1000 rpm while the mobile phase was pumped into the column in the descending mode at the flow rate used for the separation (2 mL/min). When the mobile phase emerged from the column, indicating that hydrostatic

equilibrium had been reached (back pressure : 3.7MPa), the concentrated n-hexane fraction (500mg) from 70% EtOH extract of *P. yezoensis*, which was dissolved in 6 mL of a 1:1 (v/v) mixture of the two CPC solvent system phases, was injected through the Rheodyne injection valve. The fractions were collected with 6 ml in 10 ml tube by a Gilson FC 203 B fraction collector. And the fractions from the CPC were confirmed by TLC analysis with mobile phase composed with n-hexane:EtOAc=3:1.

2. 5. HPLC–DAD–ESI/MS analysis of purified compounds

HPLC–DAD–ESI/MS analyses were carried out using a Hewlett-Packard 1100 series HPLC system equipped with an autosampler, a column oven, a binary pump, a DAD detector, and a degasser (Hewlett–Packard, Waldbronn, Germany) coupled to a Finnigan MAT LCQ ion-trap mass spectrometer (Finnigan MAT, San Jose, CA, USA) equipped with a Finnigan electrospray source and capable of analyzing ions up to m/z 2000. Xcalibur software (Finnigan MAT) was used for the operation. The chromatographic conditions are identical to those described in Section 2.4 and the outlet of the flow cell was connected to a splitting valve, from which a flow of 0.2 mL/min was diverted to the electrospray ion source via a short length of fused silica tubing. Negative ion mass spectra of the column eluate were recorded in the range m/z 100–2000. The source voltage was set to 4.5 kV and the capillary temperature to 250℃. The other conditions were as follows: capillary voltage, –36.5 V; inter-octapole lens voltage, 10 V; sheath gas, 80 psi (551.6 kPa); auxiliary gas, 20 psi (137.9 kPa).

2. 6. Cell culture and cytotoxicity assay

The murine macrophage cell line RAW 264.7 cells was grown in DMEM supplemented

with 10% (v/v) heat-inactivated FBS, penicillin (100 U/ml), and streptomycin (100 lg/ml). Cultures were maintained at 37℃ in a 5% CO_2 incubator. RAW 264.7 cells (1.5 x 10^5 cells/ml) plated in 96-well plates were pre-incubated and then treated with LPS (1 μg/ml) plus aliquots of sample at 37℃ for 24h. The medium was carefully removed from each well, and the LDH activity in the medium was determined using an LDH cytotoxicity detection kit. Briefly, 100 μl of reaction mixture were added to each well, and the reaction was incubated for 30 min at room temperature in the dark. The absorbance of each well was measured at 490 nm using a UV spectrophotometer.

2. 7. Determination of NO production

After a 24 h pre-incubation of RAW 264.7 cells (1.5×10^5 cells/ml) with LPS (1 μg/ml), the quantity of nitrite accumulated in the culture medium was measured as an indicator of NO production (%). In brief, 100 μl of cell culture medium was mixed with 100 μl of Griess reagent (1% sulfanilamide and 0.1% naphthylethylenediamine dihydrochloride in 2.5% phosphoric acid), the mixture was incubated at room temperature for 10 min, and the absorbance at 540 nm was measured in a microplate reader. Fresh culture medium was employed as a blank in every experiment. The quantity of nitrite was determined from a sodium nitrite standard curve.

2. 8. Measurement of pro-inflammatory cytokines (TNF-α, IL-1β) and PGE_2 production

All sampls were solubilized with DMSO and diluted with PBS before treatment. The inhibitory effect of samples on the pro-inflammatory cytokines (IL-1β, TNF-α) and PGE_2

875 production from LPS induced RAW 264.7 cells was determined using a competitive enzyme
876 immunoassay (ELISA) kit according to the manufacturer's instructions.
877
878 **2. 9. Western blot analysis**
879 RAW 264.7 cells plated at 2 x 10^5 cells/ml were treated with PYH5 and PYH6 purified
880 from *P. yezoensis* and harvested. The cell lysates were prepared with lysis buffer (50 mmol/l
881 Tris–HCl (pH 7.4), 150 mmol/l NaCl, 1% Triton X-100, 0.1% SDS and 1 mmol/l EDTA).
882 The cell lysates were washed via centrifugation, and the protein concentrations in the lysates
883 were determined using a BCA™ protein assay kit. The lysates containing 30 μg of protein
884 were subjected to electrophoresis on 10% or 15% sodium dodecyl sulfate–polyacrylamide
885 gels, and the gels were transferred onto nitrocellulose membranes (Bio-Rad, Hercules, CA,
886 USA). The membranes were incubated with primary antibody against COX-2, iNOS, p38,
887 phosphorylated p38 (pp38), extracellular signal-regulated kinase (ERK), phosphorylated
888 ERK (pERK), nuclear factor-kappa B (NF-$_\kappa$B) p50 and p65 and β-actin in TTBS (25 mmol/l
889 Tris–HCl, 137 mmol/l NaCl, 0.1% Tween 20, pH 7.4) containing 0.5% non-fat dry milk for 1
890 hr. The membranes were then washed with TTBS and incubated with secondary antibodies.
891 Signals were developed using an ECL Western blotting detection kit and exposed on X-ray
892 films.
893
894 **2. 8. Statistical analysis**
895 All the measurements were made in triplicate and all values were represented as means ±
896 standard error. The results were subjected to an analysis of the variance (ANOVA) using the
897 Turkey test to analyze the difference. A value of $p < 0.05$ was considered to indicate

898 statistical significance

899

900 ## 2. Results and discussion

901 ### 3. 1. NO inhibitory effects of the fractions from 70% EtOH extract of *P. yezoensis*

902 To evaluate the anti-inflammatory activity of the fractions (*n*-hexane (PYH), $CHCl_3$
903 (PYC), EtOAc (PYE) and water (PYW)) from the 70% EtOH extract of *P. yezoensis*, their
904 inhibitory activities against NO production (%) were measured in the LPS-stimulated RAW
905 264.7 cells (**Fig. 1**) and the cytotoxicity were shown in **Fig. 2**. NO production in RAW 264.7
906 cells stimulated with 1 μg/mL LPS was suppressed by the *P. yezoensis* fractions. Especially,
907 PYH showed the strongest inhibitory activity against NO production (%) comparing with the
908 other fractions and no cytotoxicity at all the concentrations.

909

910 ### 3. 2. Optimization of the two-phase solvent system

911 Partition coefficient (*K*) for the selection of a suitable two-phase solvent system was the
912 most important for the successful separation of the target samples by the preparative CPC. In
913 order to choose the most efficient separation, several two-phase solvent ratios were applied
914 with the different compositions and volume ratios of the two immiscible solvents such as *n*-
915 hexane:EtOAc:MeOH:water (v/v). The most efficient isolationcondition was then selectedas
916 9:1:9:1 (*n*-hexane:EtOAc:MeOH:water, v/v) through compare of target band size produced
917 after reaction with H_2SO_4 (**Fig. 3**). There is a great the band size gap between both top phase
918 and bottom phase of most target compounds.

919

920 ### 3. 3. Separation of compounds by CPC

The preparative CPC was operated in the Ascending mode (lower phase: stationary phase and upper phase: mobile phase, respectively) for efficiently isolation of the non-polar target compounds. The retention of the stationary phase in the coil retained 65%, and the pressure exhibited 3.7 MPa during the operation. The TLC data of vials collected through preparative CPC system was described in **Fig. 4**. We confirmed that there were six fraction (PYH1~6) including with the each same compounds and three compounds of PYH 2 were purified by preparative TLC. The HPLC-DAD-ESI/MS and NMR data of the compound in fraction B were identical to those of fucoxantin reported by Heo et al. (2009). The yields of fraction 1 ~ 6 isolated from 500 mg of the $CHCl_3$ fraction by the one-step of CPC system were 15.3 mg, 5.7 mg (PYH2-1~3: 1.2, 2.3 and 2.4 mg), 23.8 mg, 4.5 mg, 3.8 mg and 3 mg, respectively.

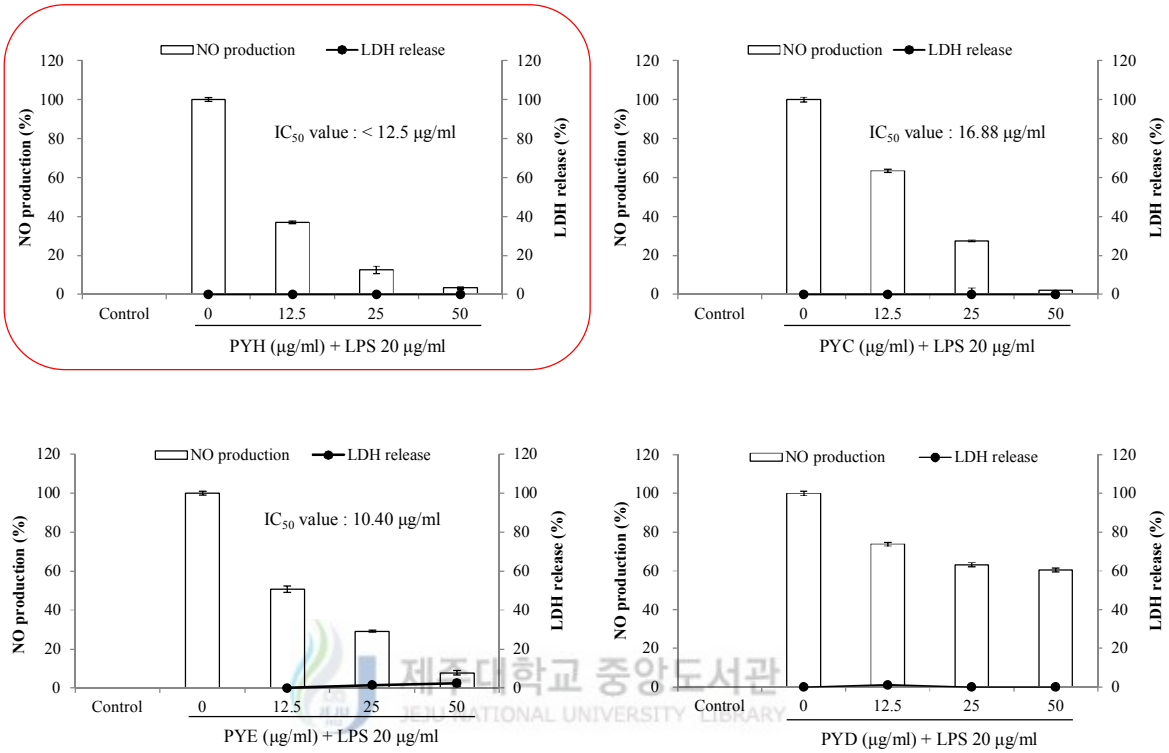

Fig. 4. NO inhibitory effects of the fractions from 70% EtOH of *P. yezoensis* in LPS-induced RAW 264.7 cells

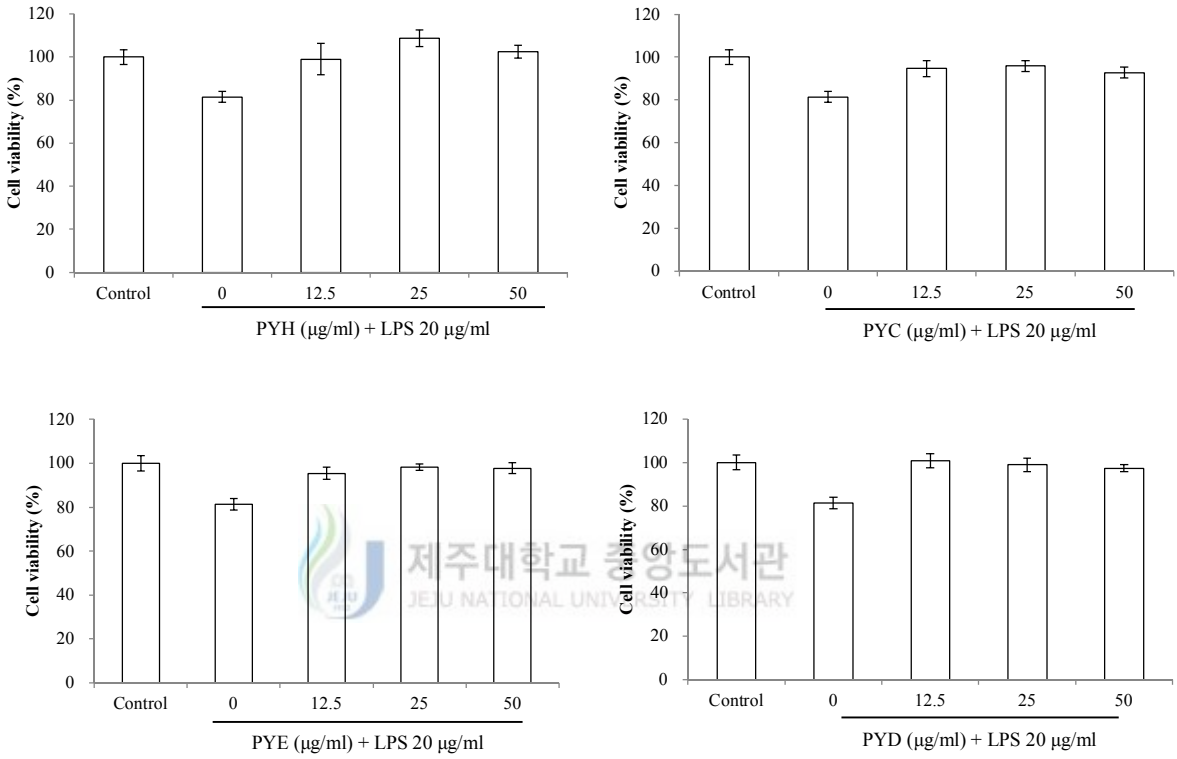

Fig. 5. Cytotoxicity of the fractions from 70% EtOH of *P. yezoensis* in LPS-induced RAW 264.7 cells

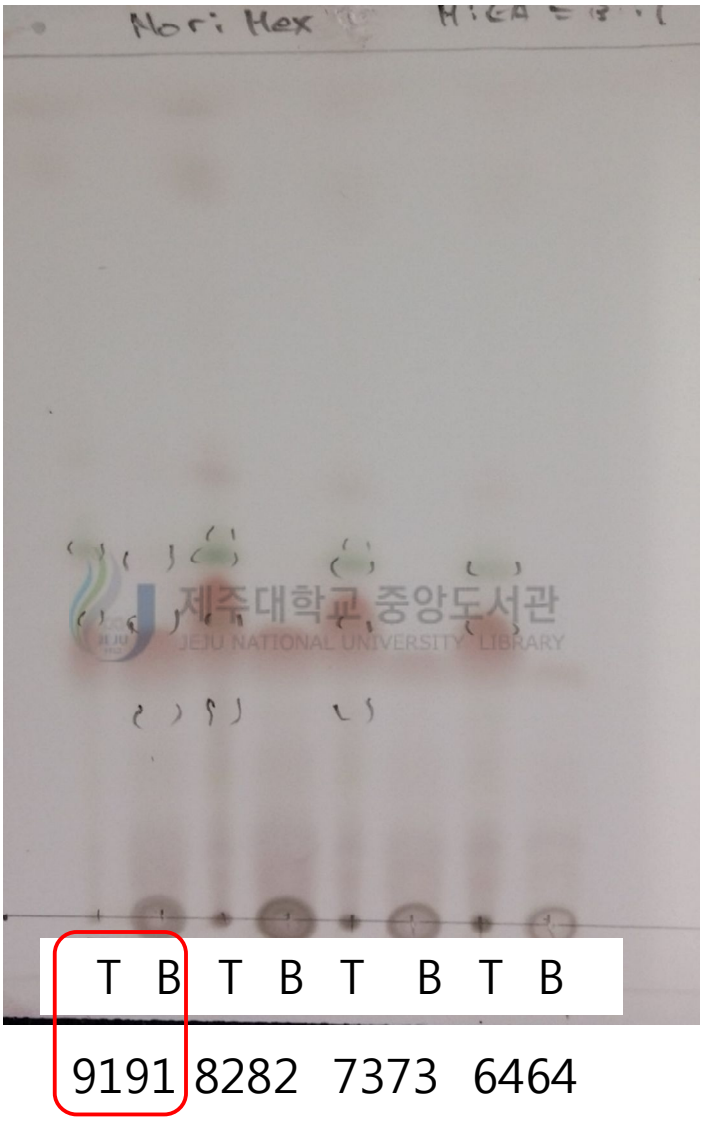

Fig. 6.TLC analysis data of n-hexane fraction from 70% EtOH extract to efficiently operate the preparative CPC

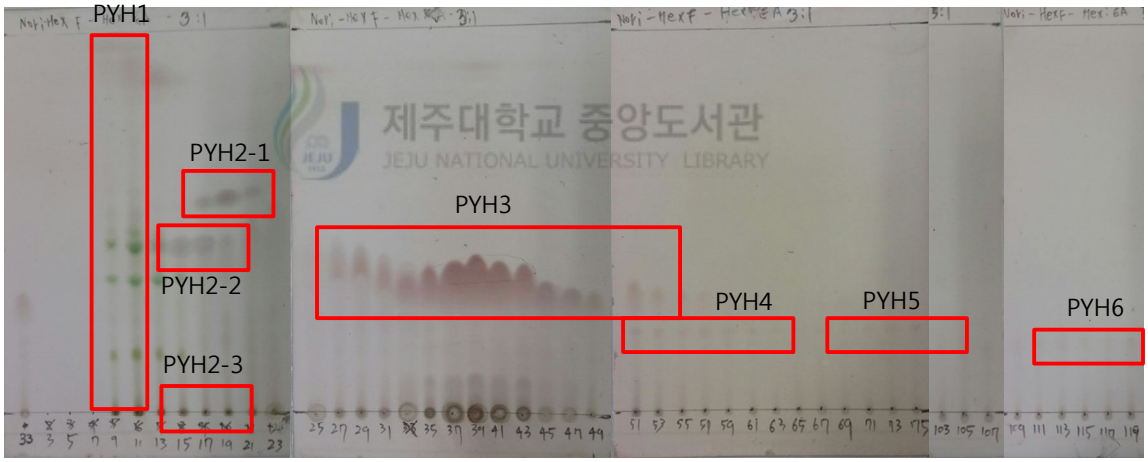

Fig. 7.TLC analysis data of the CPC fractions from n-hexane fraction

3. 4. NO inhibitory effects of the compounds from n-hexane fraction of *P. yezoensis*

To evaluate the anti-inflammatory activity of the compounds isolated from the n-hexane fraction of *P. yezoensis*, the inhibitory activity against the NO production (%) were measured in the LPS induced 267.4 RAW cells (**Fig. 5**). RAW 264.7 cells treated with the compounds for 2h were then stimulated with 1 μg/ml LPS for the 24 h incubation. The culture supernatants were used for the evaluation of NO production by Griess reaction. PYH 5and 6 showed the excellent inhibitory activity against NO production (%) and their cytotoxicity did not show at below 25 μg/ml, therefore all following experiments were progressed at concentrations below 25 μg/ml.

3. 5. Structural identification of anti-inflammatory compounds

The identification of PYH5 and 6 among the CPC fractions was carried out by ^{1}H NMR, ^{13}C NMR and HPLC–DAD–ESI/MS (positive ion mode). PYH5 and 6were confirmed as (11Z,13E,15E)-17-(5-hydroxycyclohexa-1,3-dienyl)heptadeca-11,13,15-trien-2-oneand 1-ethyl-3-(3-(3-methylbutan-2-yl)-14-phenyltetra -decyl)benzene, respectively (**Fig. 6**).

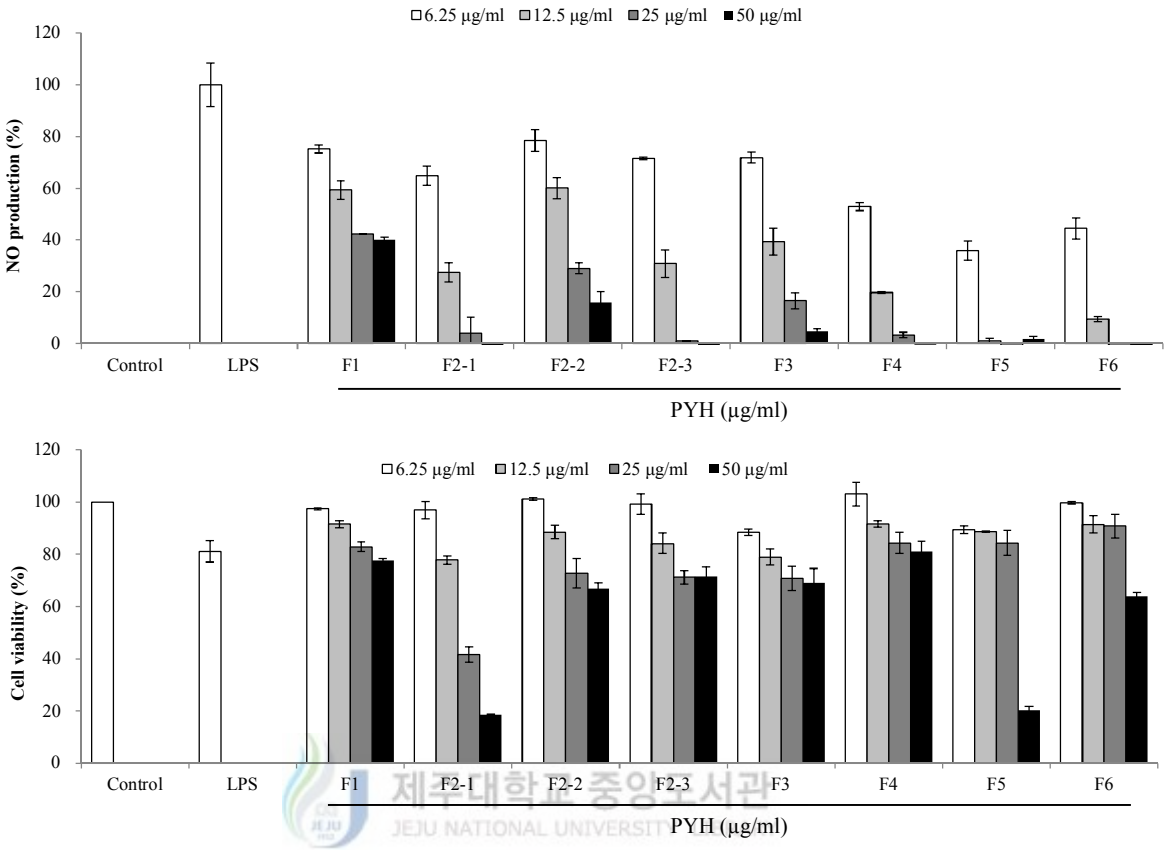

Fig. 8.NO inhibitory effects and cytotoxicity of the CPC fractions in LPS-induced RAW 264.7 cells

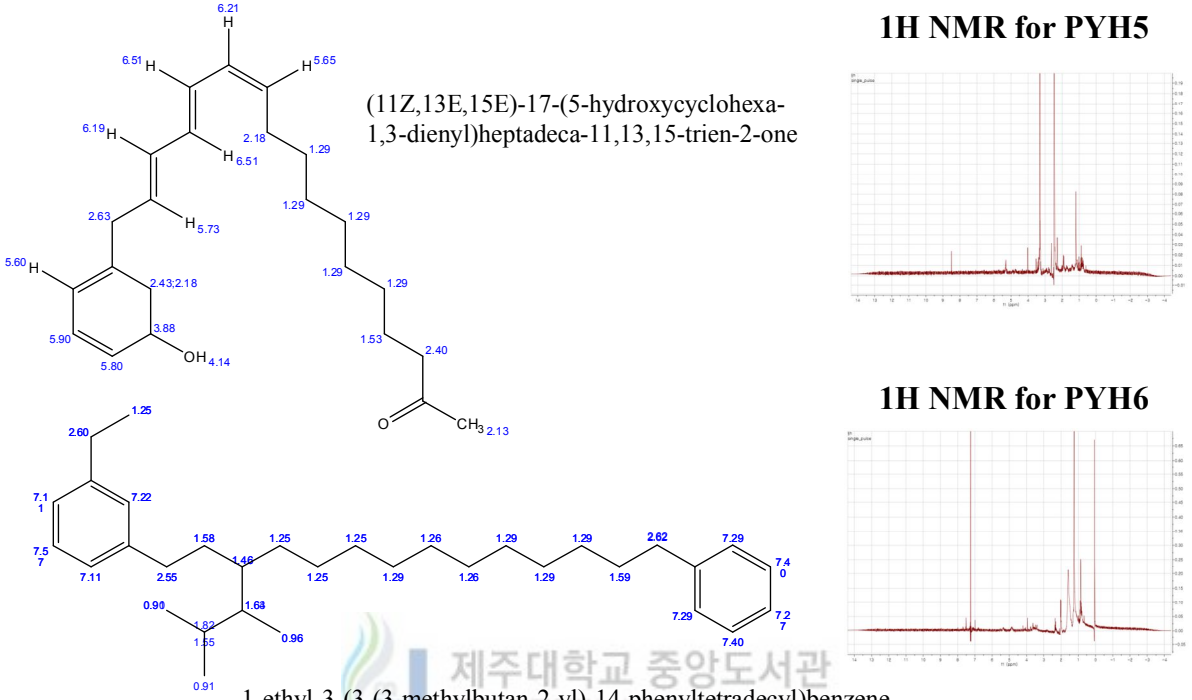

Fig. 9. Chemical structures and proton NMR data of PYH5 and 6

3. 6. PYH5 inhibited release of PGE_2,and protein expression of COX-2 and iNOS in

LPS-induced RAW 264.7 macrophages

The production of $PGE_2$was significantly increased upon the LPS treatment when compared with the untreated control group. However, PYH5 dose-dependently decreased the LPS-stimulated PGE_2 production (**Fig. 7(A)**). The protein expression of COX-2 and iNOS were significantly increased upon the LPS treatment when compared with the untreated control group. However, PYH5 prominently suppressed the LPS-stimulated COX-2 and iNOS protein expression in a dose dependent manner (**Fig. 8**).

3. 7. PYH5 decreased pro-inflammatory cytokines released by LPS-stimulation in RAW 264.7 macrophages

The pro-inflammatory cytokines produced from macrophages, are the key components of inflammation. Therefore, the effect of PYH5 on the production levels of the inflammatory cytokines TNF-α and IL-1ß were investigated by ELISA kit using the conditioned media of LPS-stimulated RAW 264.7 macrophages. The LPS stimulation significantly increased the production of pro-inflammatory cytokines TNF-α and IL-1ß compared to the non-stimulated blank groups. The LPS induced production of TNF-α and IL-1ß showed a significant concentration dependent decrease following the treatment of **PYH5** (**Fig. 7(B) and (C)**).

3. 8. PYH5 affected phosphorylation of NF-κB and MAPK in LPS-induced RAW 264.7 macrophage

Phosphorylation of NF-κB, $ERK_{1/2}$, and p38 MAPK were caused by LPS-stimulation within 15 min in macrophage RAW 264.7 cells. However, PYH5 significantly suppressed the phosphorylation of $ERK_{1/2}$whereasdidn't affect to p38 MAPK.PYH5strongly reduced the

phosphorylation of NF-κBin the cytosol of the LPS-stimulated macrophages (**Fig. 9 and 10**). These results exhibited that PYH5 might effectively block NF-κB and MAPK signal transduction in the activated macrophage RAW 264.7 cells.

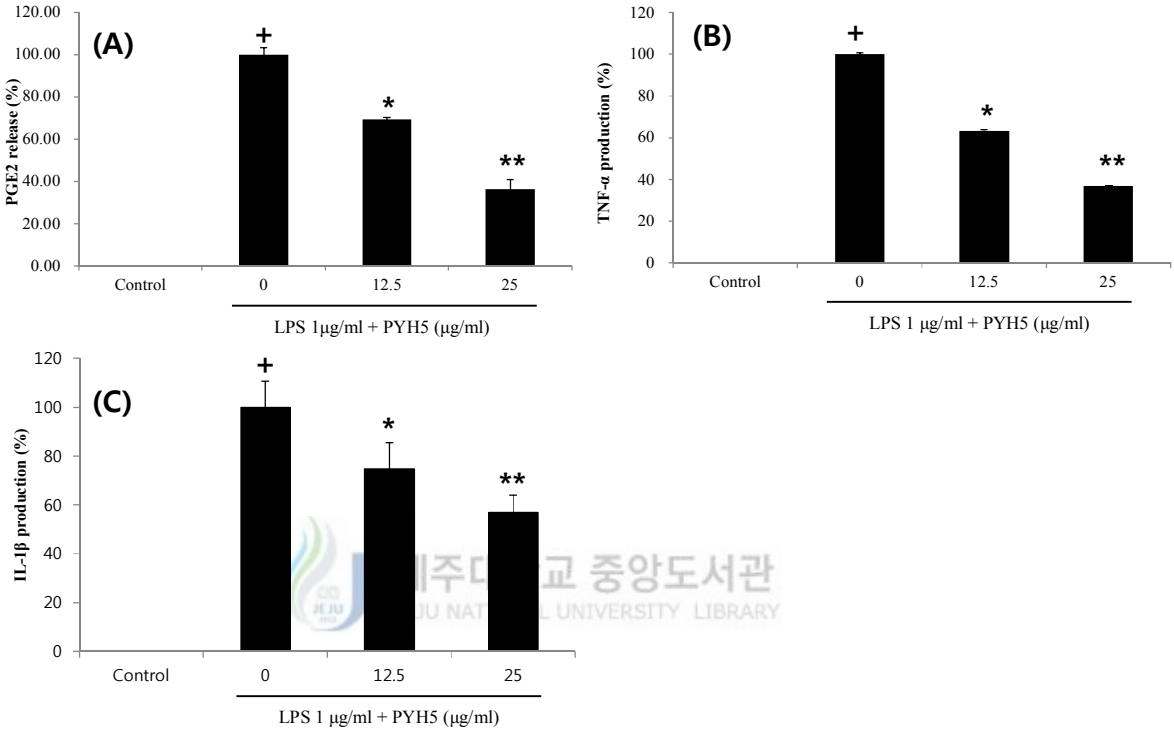

Fig. 10. Pro-inflammtory cytokines inhibitory effect of PYH5 from the n-hexane fraction in LPS-induced RAW 264.7 cells. (A) PGE2, (B) TNF-α, and (C) IL-1β.

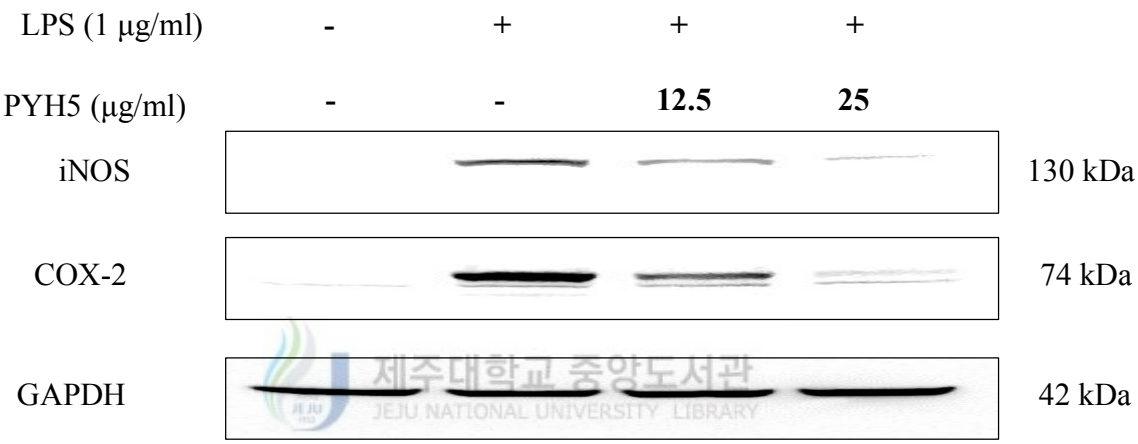

Fig. 11. Pro-inflammatory protein inhibitory effect of PYH5 from the n-hexnae fractions in LPS-induced RAW 264.7 cells

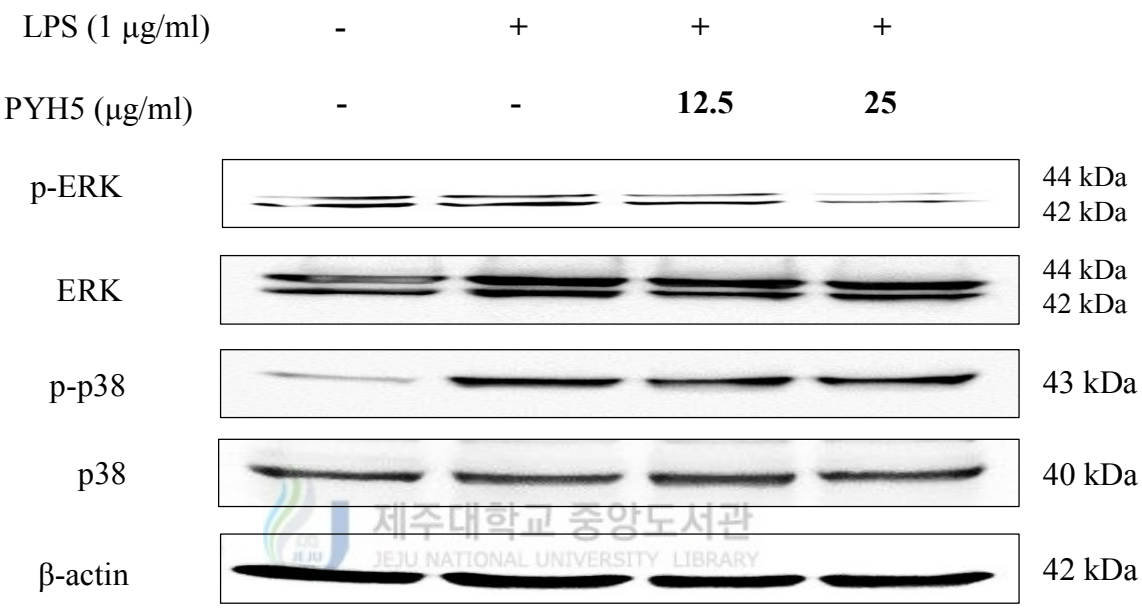

Fig. 12. MAPKs proteins inhibitory effect of PYH5 from the n-hexnae fractions in LPS-induced RAW 264.7 cells

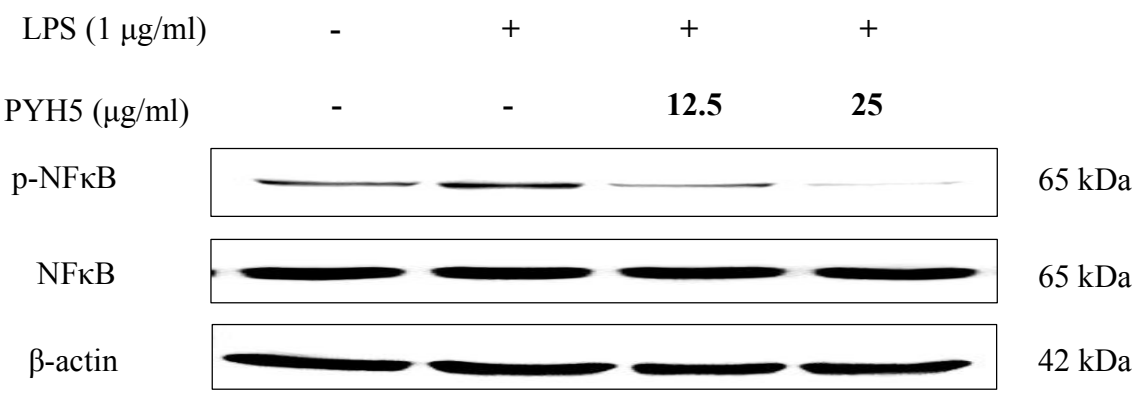

Fig. 13. NF-κB proteins inhibitory effect of PYH5 from the n-hexnae fractions in LPS-induced RAW 264.7 cells

3. 9. PYH6 inhibited release of PGE_2, and protein expression of COX-2 and iNOS in LPS-induced RAW 264.7 macrophages

The production of PGE_2 was significantly increased upon the LPS treatment when compared with the untreated control group. However, PYH6 dose-dependently decreased the LPS-stimulated PGE_2 production (**Fig. 11(A)**). The protein expressions of COX-2 and iNOS were significantly increased upon the LPS treatment when compared with the untreated control group. However, PYH6 prominently suppressed the LPS-stimulated COX-2 and iNOS proteins expression in a dose dependent manner (**Fig. 12**).

3. 5. PYH6 decreased pro-inflammatory cytokines released by LPS-stimulation in RAW 264.7 macrophages

The pro-inflammatory cytokines produced from macrophages, are the key components of inflammation. Therefore, the effect of PYH6 on the production levels of the inflammatory cytokines TNF-α and IL-1ß were investigated by ELISA kit using the conditioned media of LPS-stimulated RAW 264.7 macrophages. The LPS stimulation significantly increased the production of pro-inflammatory cytokines TNF-α and IL-1ß compared to the non-stimulated blank groups. The LPS induced production of TNF-α and IL-1ß showed a significant concentration dependent decrease following the treatment of PYH6 (**Fig. 11(B) and (C)**).

3. 6. PYH6 affected phosphorylation of NF-κB and MAPK in LPS-induced RAW 264.7 macrophage

Phosphorylation of NF-κB, $ERK_{1/2}$, and p38 MAPK were caused by LPS-stimulation within 15 min in macrophage RAW 264.7 cells. However, PYH6 significantly suppressed the phosphorylation of $ERK_{1/2}$and p38 MAPK whereasdidn't affect to the phosphorylation of NF-κB in the cytosol of the LPS-stimulated macrophages (**Fig. 13 and 14**). These results

exhibited that PYH6 might effectively block MAPK signal transduction in the activated macrophage RAW 264.7 cells.

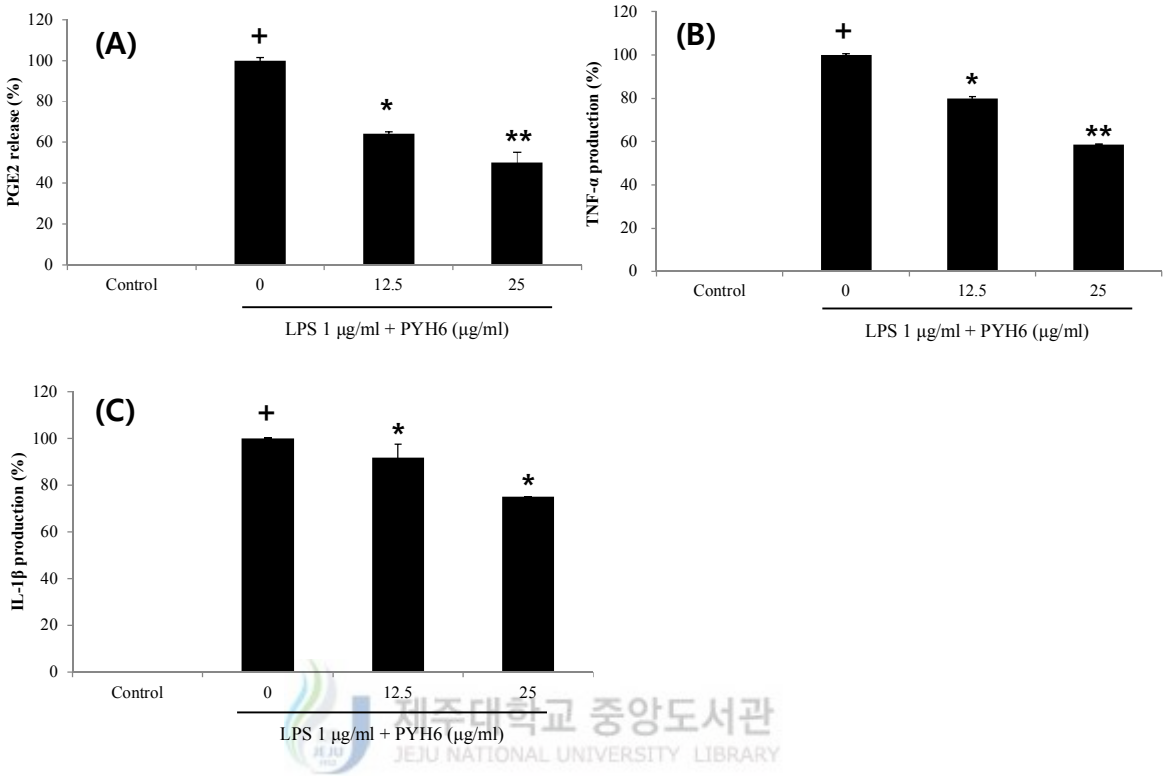

Fig. 14. Pro-inflammtory cytokines inhibitory effect of PYH6 from the n-hexane fraction in LPS-induced RAW 264.7 cells.(A) PGE2, (B) TNF-α, and (C) IL-1β.

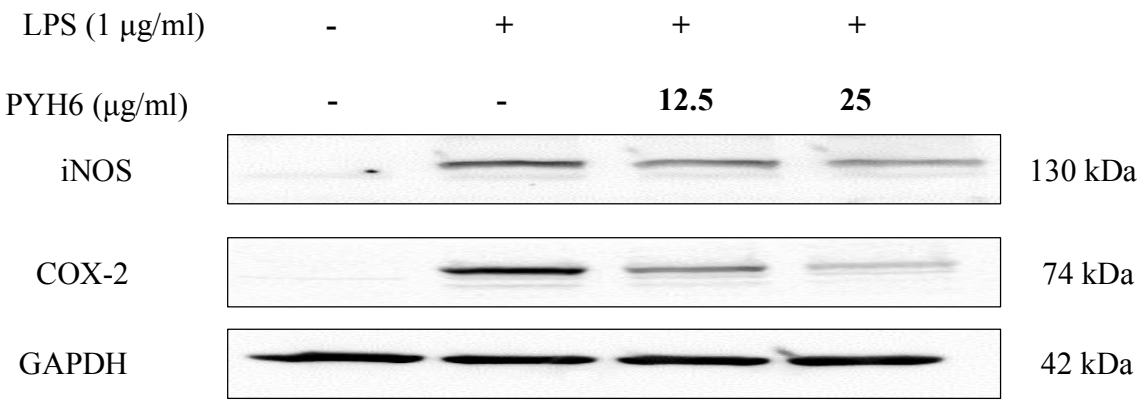

Fig. 15. Pro-inflammatory protein inhibitory effect of PYH6 from the n-hexnae fractions in LPS-induced RAW 264.7 cells

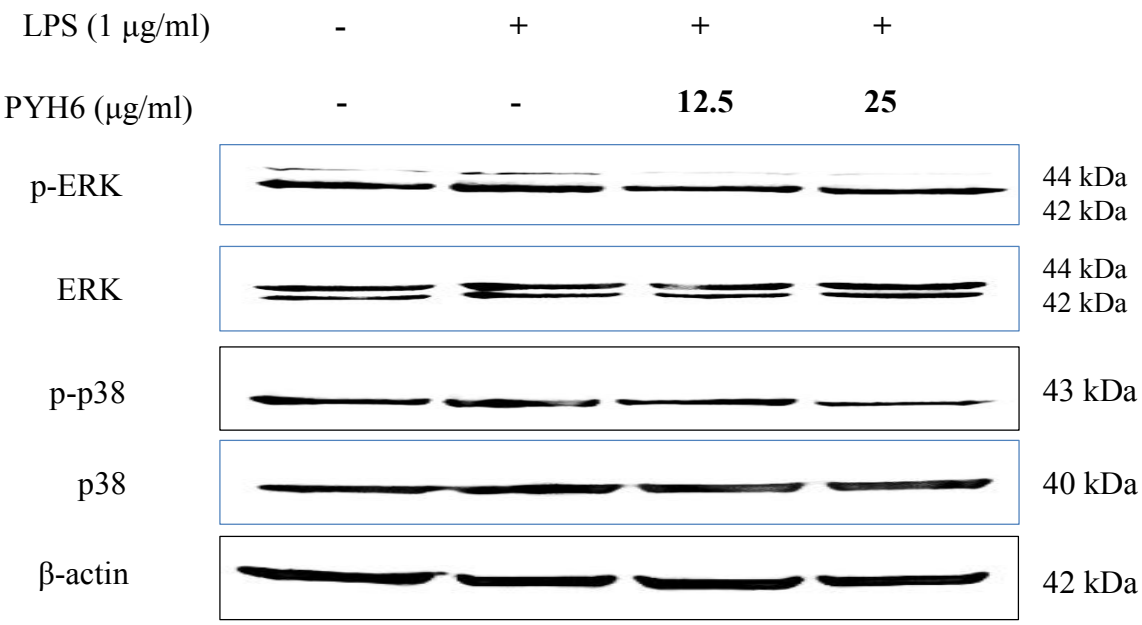

Fig. 16. MAPKs proteins inhibitory effect of PYH6 from the n-hexnae fractions in LPS-induced RAW 264.7 cells

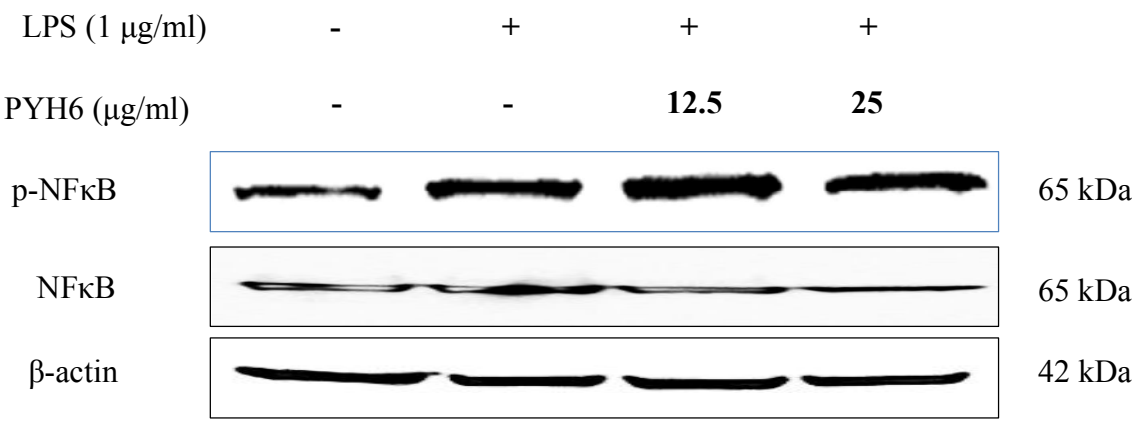

Fig. 17. NF-κB proteins inhibitory effect of PYH6 from the n-hexnae fractions in LPS-induced RAW 264.7 cells

Part-III

Potential anti-diabetes compound from *Pyropia yezoensis*, a marine red alga regulates glucose transporter, GLUT-4 translocation through AKT and AMPK pathways

Abstract

This study demonstrated on anti-diabetes mechanism of compounds from *Pyropia yezoensis*,a marine red alga.Among the fractions (*n*-hexane (PYH), $CHCl_3$ (PYC), EtOAc (PYE) and water (PYW)) from the 70% EtOH extract of *P. yezoensis*, PYH showed the strongest inhibitory activity on α-glucosidase (%) comparing with the other fractions. And (E)-5-(8-hydroxynon-6-enyl)cyclohexa-2,4-dienol (C24D) among seven compounds from PYH showed the strongest inhibitory activity on α-glucosidase as well as increased glucose uptake level without cytotoxicity on C2C12 mouse muscle cells, whereas other six compounds didn't affect to glucose uptake at all concentrations.Glucose transpotor, GLUT4 was controlled by AKT and AMPK pathways, so we evaluated role of C24D for AKT and AMPK pathways. Insulin only upregulated the phosphor-AKT protein, whereas C24Dincreased the activation of phosphor-AKT and -AMPK proteins, also PI3K and AMPK inhibitors restricted the GLUT-4 expression in cytosol of C2C12 under the treatment of C24D. *In vivo* results, the blood glucose level in zebrafish which damaged by alloxan slightly was decreased whereas, C24Dstrongly decrease the level of blood glucose level. Thus, blood

glucose level increased in alloxan damaged zebrafish by administration of starch was regulated by C24D. Consequently, (E)-5-(8-hydroxynon-6-enyl)cyclohexa-2,4-dienol was main agent of anti-diabetes in *P. yezoensis*. And we suggest that C24D inhibits the activation of glucosidase *in vitro* and *in vivo* and regulates the GLUT-4 via AKT and AMPK pathways.

1. Materials and methods

2. 1. Inhibition assay for α-glucosidase activity

The α-glucosidase inhibitory assay was done by the chromogenic method described by Watanabe et al., (1997) using a readily available yeast enzyme. Briefly, yeast α-glucosidase (0.7 U, Sigma) was dissolved in 100 mM phosphate buffer (pH 7.0) containing 2 g/l bovine serum albumin and 0.2 g/l NaN_3 and used as an enzyme solution. 5 mM p-Nitrophenyl-α-D-glucopyranoside in the same buffer (pH 7.0) was used as a substrate solution. The 50 μl of enzyme solution and 10 μl of sample dissolved in dimethylsulfoxide were mixed in a microtiter plate and measured absorbance at 405 nm at zero time. After incubation for 5 min, substract solution (50 μl) was added and incuvated for another 5 min at room temperature. The increase in the absorbance from zero time was measured. Percent inhibitory activity was expressed as 100 minus relative absorbanve difference (%) of test compounds to absorbance change of the control where test solution was replaced by carrier solvent.

2. 2. Cell culture

Mouse myoblast C2C12 cells were maintained in high glucose-DMEM supplemented with 10% heat-inactivated FBS, penicillin (100 U/ml) and streptomycin (100 μg/ml).

Cultures were maintained at 37℃ in 5% CO_2incubator.For differetiationm the cells were seeded in appropriate culture plates, and after sub-confluence (about 80%), the medium was changed to DMEM containing 2% horse serum for 7 days, with medium changes every day. All experiments were performed in differentiated C2C12 myotubes after 7 days.

2. 3. Glucose uptatke assay

C2C12 cells were seeded in a 24-wells plate. After differentiation, the cells were starved in serum-free low glucose DMEM for 12 h, and then washed with PBS and incubated with fresh serum-free low glucose DMEM. After that, the cells were treated without or with 100 μg/ml of samples for 3 h. Glucose uptake was measured by glucose concentration in the media solution using glucose oxidase assay kit (Asan Pharmaceutical corp., Korea).

2. 4. Experimental animals

Adult zebrafish were obtained from a commercial dealer (Seoul Aquarium, Seoul, Korea) and 15 fishes were kept in a 3.5 L acrylic tank under the following conditions; 28.5 ± 1 oC, and fed twice a day (Tetra GmgH D-49304 Melle Made in Germany) with a 14/10 h light/dark cycle. The zebrafish were exposed of 2 mg/mL alloxan for 1 h and transferred to 1% glucose during 1 h. And then, the solution was changed to water for 1 h. The zebrafish were anesthetized using 2-phenoxy ethanol (1:1000 dilution). The zebrafish were divided to 4 groups, the normal (alloxan-untreated) as well as alloxan-induced diabetic zebrafish without (control) and with PYH4 or Metformin(Met) (1 μg/g body weight).

2. 5. Measurement of blood glucose level

The Zebrafish was anesthetized by 2-phenoxy ethanol and removed from the water by Kimwipe. After, blood sample was taken from the heart at 0, 60, 90, 120 min. Approximately 1 μL of blood rapidly transferred to a glucometer strip (Roche Diagnostics Gmbh, Germany).

2. Results and discussion

3. 1. α-glucosidase inhibitory effect of the fractions from 70% EtOH extract of *P. yezoensis*

The α-glucosidase inhibitory activities of the fractions (*n*-hexane (PYH), $CHCl_3$ (PYC), EtOAc (PYE) and water (PYW)) from the 70% EtOH extract of *P. yezoensis* were showed in **Fig. 15**. PYH showed the strongest inhibitory activity against α-glucosidase (%) comparing with the other fractions and its IC_{50} value was 0.512 mg/ml.

3. 2. α-glucosidase inhibitory effects of the compounds from n-hexane fraction of *P. yezoensis*

To evaluate the α-glucosidase inhibitory activity of the compounds isolated from the n-hexane fraction of *P. yezoensis*, the inhibitory activity against the α-glucosidase (%) were measured by diminishing the absorption of glucose decomposed from starch by these ezymes (Hara and Honda, 1990) (**Fig. 16**). PYH4 among seven compounds (PYH2-1~6) from PYH showed the strongest inhibitory activity against α-glucosidase (%) whereas other six compounds showed very low inhibitory activities of below 50% at all concentrations. Also, PYH4 extremely inhibited α-glucosidae comparing with positive control, acarbose.

3. 3. Glucose uptake effects of the compounds from n-hexane fraction of *P. yezoensis*

To evaluate the glucose uptake activity of the compounds isolated from the n-hexane fraction of *P. yezoensis*, the inhibitory activity against the α-glucosidase (%) were measured by glucose concentration in the media solution using glucose oxidase assay kit (Asan Pharmaceutical corp., Korea) (**Fig. 17**). PYH4 among seven compounds (PYH2-1~6) from PYH showed the strongest activity of glucose uptake without cytotoxicity on C2C12 cells, whereas other six compounds didn't affect to glucose uptake at all concentrations.

3. 4. Structural identification of α-glucosidase inhibitory compounds

The identification of PYH4 among the CPC fractions was carried out by ^{1}H NMR, ^{13}C NMR and HPLC–DAD–ESI/MS (positive ion mode). PYH4 was confirmed as (E)-5-(8-hydroxynon-6-enyl)cyclohexa-2,4-dienol (**Fig. 18**).

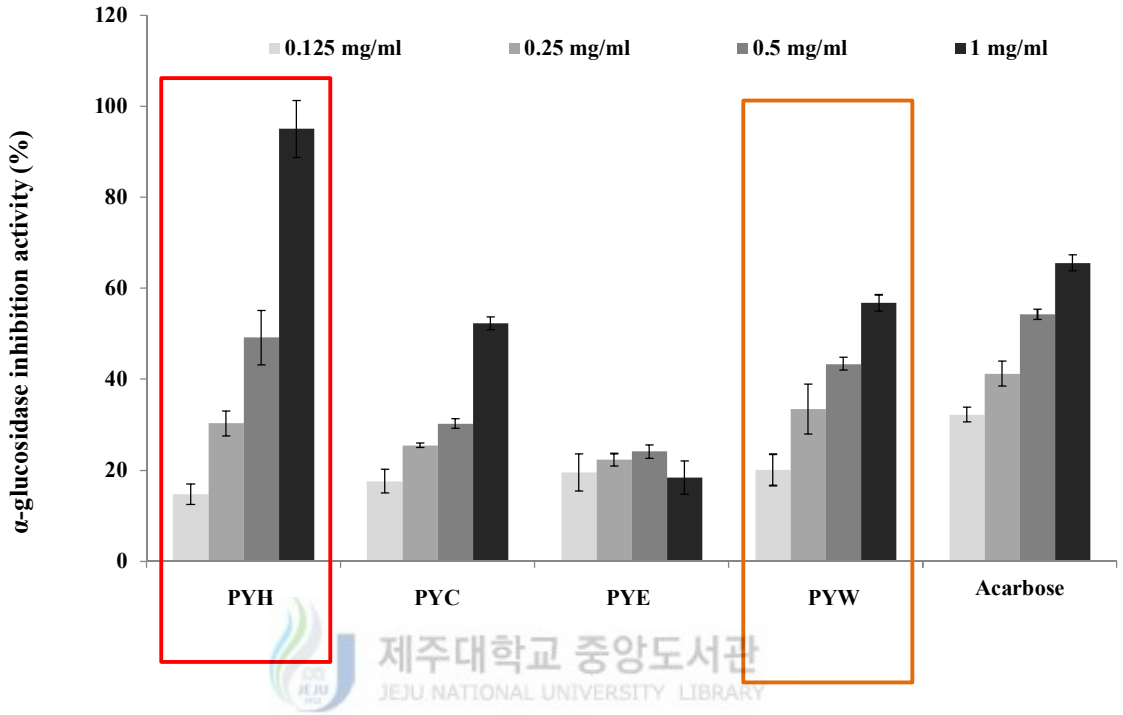

Fig. 18.α-glucosidase inhibitory effects of the fractions from 70% EtOH extract of *P. yezoensis*

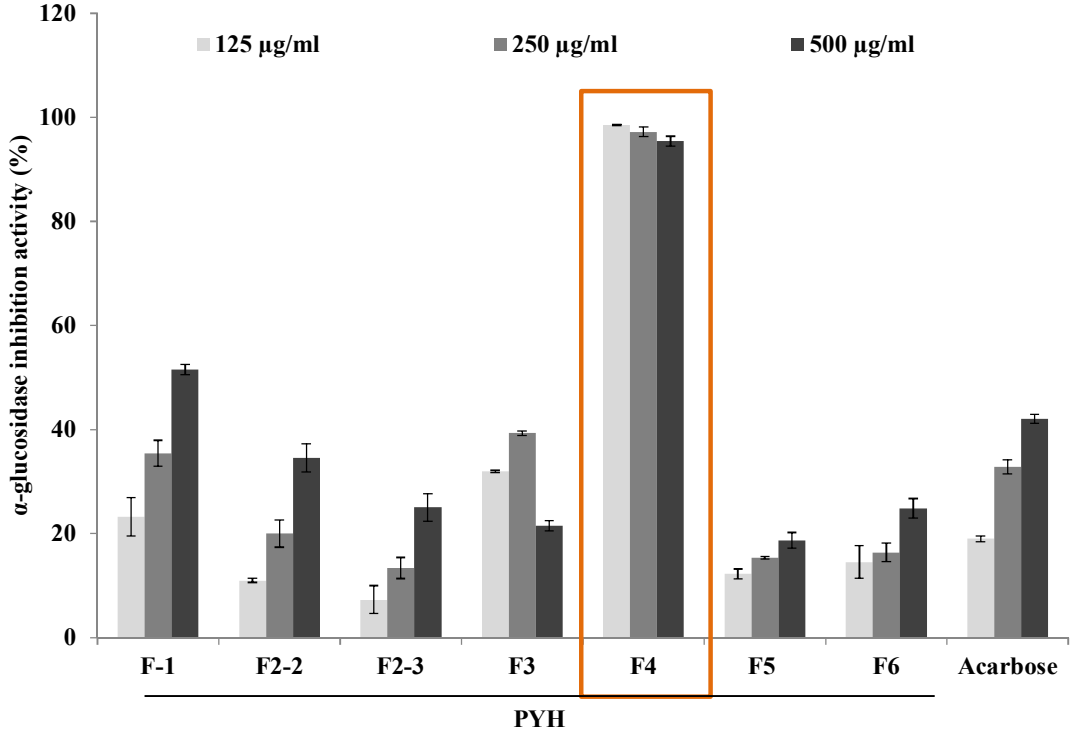

IC_{50} (mg/ml)	0.47	>0.5	>0.5	>0.5	<0.13	>0.5	>0.5	>0.5

Fig. 19.α-glucosidase inhibitory effects of the CPC fractions from n-hexane of *P. yezoensis* and their IC_{50} values

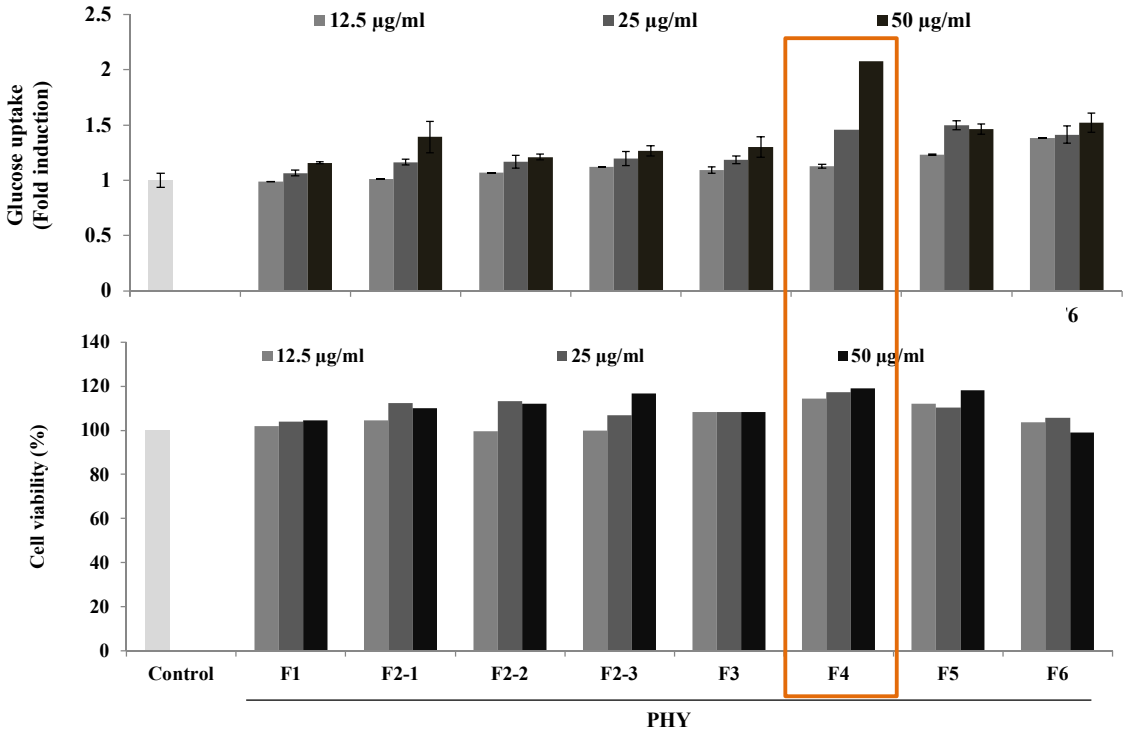

Fig. 20. Glucose uptake effects of the CPC fractions from n-hexane of *P. yezoensis* in C2C12 mouse muscle cells.

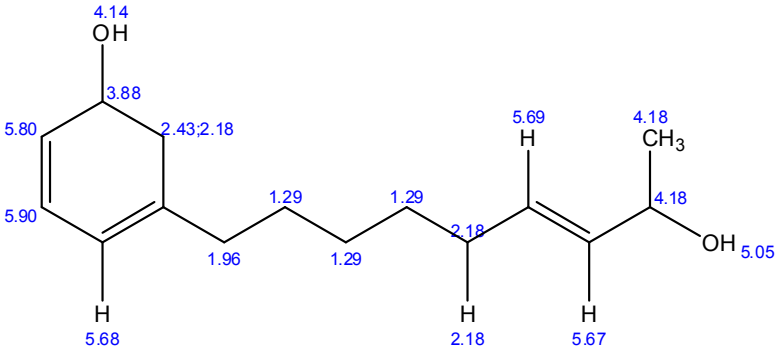

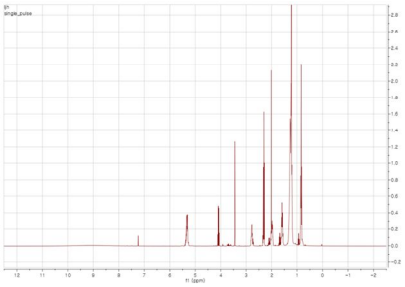

1H NMR for PYH4

(E)-5-(8-hydroxynon-6-enyl)cyclohexa-2,4-dienol

Fig. 21. Chemical structure and proton NMR data of PYH4 from *P. yezoensis*.

3. 5. α-glucosidase inhibitory effect of PYH4 from *P. yezoensis*

The α-glucosidase inhibitory activities of PYH4 as increase of the concentration were showed in **Fig. 19**. The positive control, acarbose showed α-glucosidase inhibitory activities of below 50% in all concentrations whereas PYH showed very strong inhibitory activity against α-glucosidase (%)and its IC_{50} value was 74μg/ml.

3. 6. Change of blood glucose levelbyPYH4 in alloxan stimulated diabetic zebrafish

The change of level of glucose in the blood byPYH4 isolated from the n-hexane fraction of *P. yezoensis*on Alloxane stimulated diabetic zebrafish model, exhibited in **Fig. 20**. The blood glucose level of control group was slightly decreased as increase of time whereas PYH4 similarly decreased the glucose level of blood with positive control, metformin.

3. 7. Glucose uptake effect of PYH4via AKT and AMPK pathways

The glucose uptake is generated by activation of glucose transporter, GLUT4 via AKT and AMPK pathways. Insulin (INS) induced the strong expression of phosphor-AKT protein whereas didn't affect to expression of phosphor-AMPK protein. PYH4 increased the expression of phosphor-AMPK and AKT proteins in dose dependent manners (**Fig. 21**).

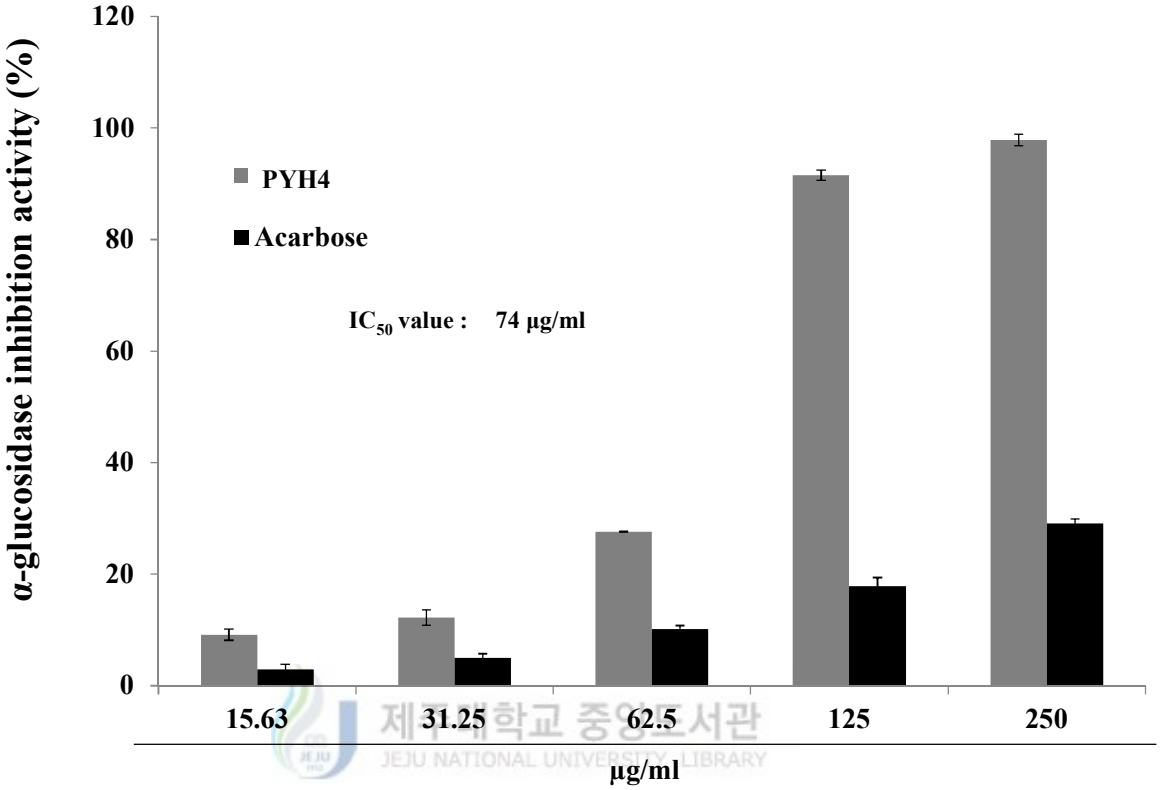

Fig. 22.α-glucosidase inhibitory effects of PYH4 from n-hexane of *P. yezoensis*.

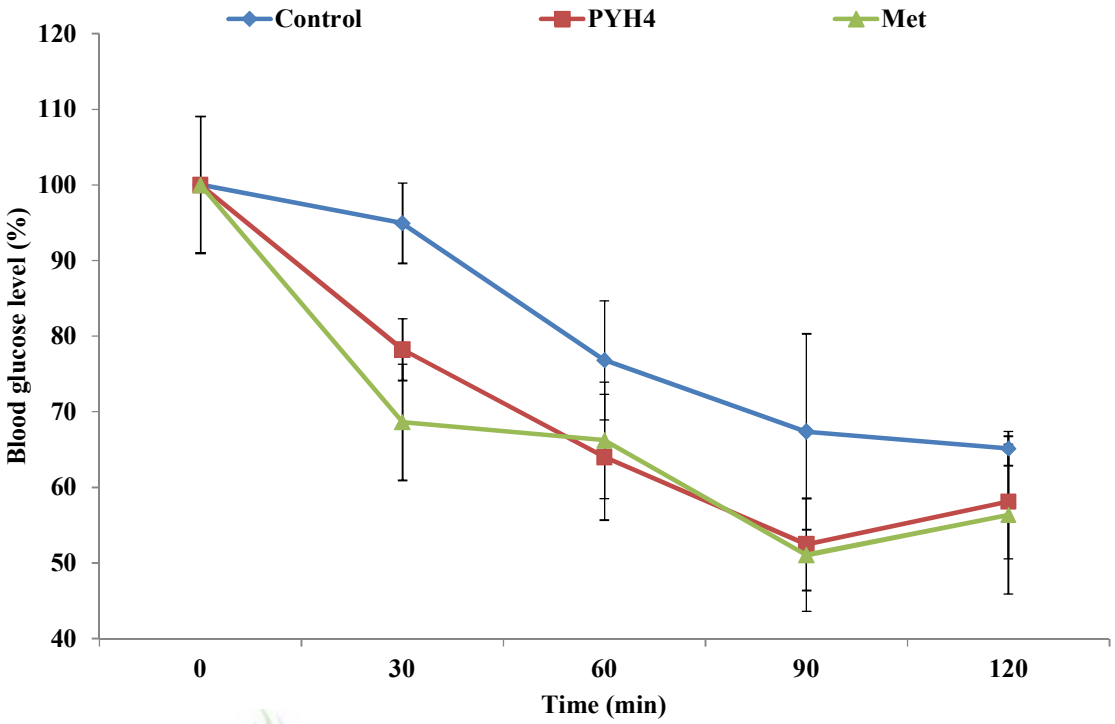

Fig. 23. Blood glucoselevel inhibitory effect of PYH4 from n-hexane of *P. yezoensis*in alloxan stimulated zebrafish

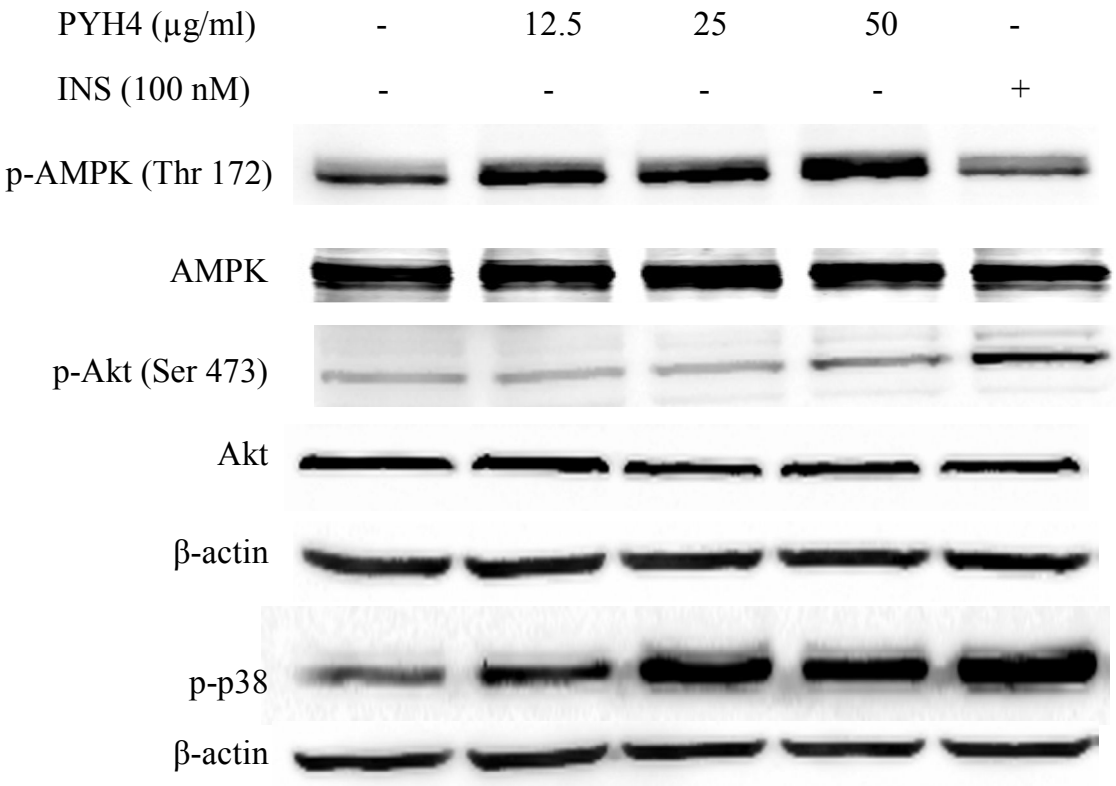

Fig. 24. Expression effects of PYH4 from n-hexane of *P. yezoensis* on AMPK and AKT proteins

Part-V

Development of liver inflammatory and cirrhosis models of adult zebrafish induced by ethanol and CCl_4

1. Abstract

This study focus on development of liver cirrhosis model of zebrafish by ethanol (EtOH) and CCl_4. 1% EtOH strongly affected the liver damage however didn't generated the liver cirrhosis mediator during 3 weeks. CCl4 induced the liver damage and inflammation, and especially expressed TGF-β1. PYH5 and 6 extremely decreased the ethanolic live damage and inflammation of zebrafish. Especially, PYH5 showed very strong anti-inflammatory effect. Consequently, 1% EtOH didn't enough to induced the liver cirrhosis on zebrafish for 3 weeks, whereas CCl4 induced strongly potentially liver cirrhosis. Also, PYH5 and 6 are useful good agents for anti-inflammatory and anti-liver cirrhosis.

2. Materials and methods

2. 1. Experimental animals

Adult zebrafish were obtained from a commercial dealer (Seoul Aquarium, Seoul, Korea) and 15 fishes were kept in a 3.5 L acrylic tank under the following conditions; 28.5 ± 1 oC, and fed twice a day (Tetra GmgH D-49304 Melle Made in Germany) with a 14/10 h light/dark cycle.

2. 2. Development of potentially ethanolic cirrhosis model of zebrafish

1% ethanol (EtOH) administratedto zebrafish once a day and, before administration of 1% EtOH, water was changed day by day. The zebrafishes were divided to 6 groups with normal, EtOH administrated, EtOH and PYH5 low dose, EtOH and PYH5 high dose, EtOH

and PYH6 low dose, and EtOH and PYH6 high dose groups. After that zebrafishes were anesthetized using 2-phenoxy ethanol (1:1000 dilution), the samples were injected to high dose (12.5 μg/g of zebrafish) and low dose (6.25 μg/g of zebrafish) and all process was shown in **Fig. 22 (A)**.

2. 3. Development of potentiallychemical cirrhosis model of zebrafish

10% CCl_4 administrated to zebrafish twice a week and, before administration of 10% CCl_4, water was changed day by day. The zebrafishes were divided to 6 groups with normal, CCl_4 administrated, CCl_4 and PYH5 low dose, CCl_4 and PYH5 high dose, CCl_4 and PYH6 low dose, and CCl_4 and PYH6 high dose groups. After that zebrafishes were anesthetized using 2-phenoxy ethanol (1:1000 dilution), the samples were injected to high dose (12.5 μg/g of zebrafish) and low dose (6.25 μg/g of zebrafish) all process was shown in **Fig. 22 (B)**..

2. 3. Collection of liver of zebrafish

After that zebrafishes were anesthetized using 2-phenoxy ethanol (1:1000 dilution), performed a laparotomy of zebrafish. And then did a resection of liver in zebrafish. The resected liver was immediately kept in -70℃ refrigerator.

2. 3. RNA Preparation.

The tissue were obtained and lysed in the Trizol reagent (Molecular Research Center, Cincinnati, OH). The addition of chloroform (Sigma-Aldrich) and incubation for 5 min at 4°C followed. Supernatants obtained after centrifugation were mixed with isopropanol (Sigma), and the resulting RNA pellets were washed with EtOH and stored at −20°C until

use.

2. 4. Reverse Transcriptase-Polymerase Chain Reaction (RT-PCR).

The cDNA was synthesized with RNA purified from zebrafish liver via an Advantage RT-for-PCR kit, according to manufacturer's instructions (Clontech Laboratories, Inc. A Takara Bio company, Japan). PCR of this cDNA and the primer (Cosmo genetech, South Korea), shown in **Table 1**, was performed for 50 cycles with a 5-min denaturing step at 94°C, a 1-min annealing step at 55 to 62°C, and a 20-min extension phase at 72°C using the Roche Light cycler 480 PCR machine (Roche, Germany).

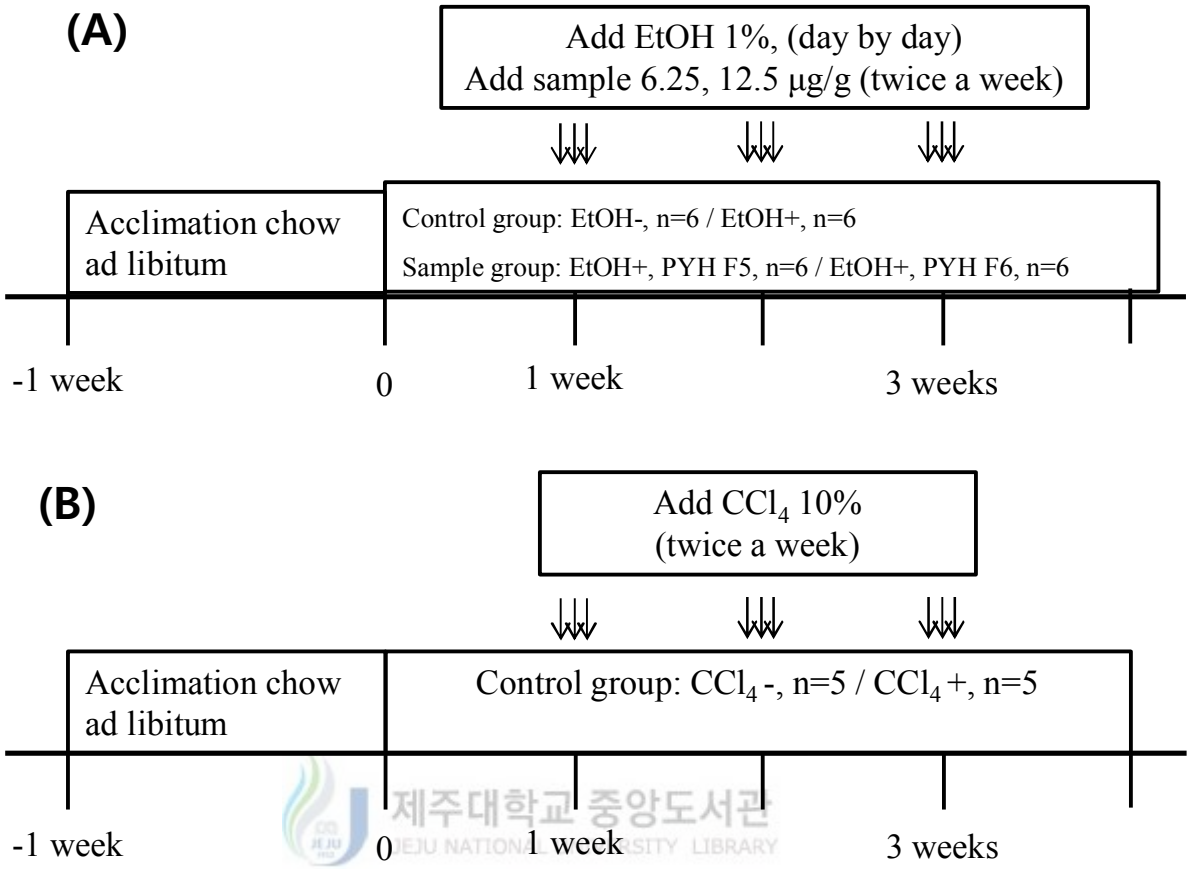

Fig. 25. Diagram for potentially ethanolic cirrhosis model development of zebrafish

Table 6. Sequences and expected sizes of cytokine primers for RT-PCR used in this study

Oligonucleotide	Sequence		Expected size (bp)
β-Actin	5'-Primer	GCTGACAGGATGCAGAAGAA	200
	3'-Primer	TAGAAGCATTTGCGGTGGAC	
IL-1β	5'-Primer	TTGTGGGAGACAGACAGTGC	191
	3'-Primer	GATTGGGGTTTGATGTGCTT	
TNF-α	5'-Primer	ACAAGGCAATTTCACTTCCA	194
	3'-Primer	AGCTGATGTGCAAAGACACC	
iNOS	5'-Primer	GAGCAGGCCCAATGCATTT	186
	3'-Primer	TGCGCTGCTGCCAGAAAC	
IL-6	5'-Primer	TCAACTTCTCCAGCGTGATG	21
	3'-Primer	TCTTTCCCTCTTTTCCTCCTG	
TGF β1	5'-Primer	CGACTGTAAAGCAAACCAGCAGAGCACG	31
	3'-Primer	GTGTCCTCCCATTGAGATGTTATGTATGTCC	

3. Results

3. 1. Hepatoprotective effectof PYH5 and 6 in ethanol damaged liver of adult zebrafish

EtOH treated group increased the death of zebrafish whereas treatments of PYH5and 6 decreased the death rate of 10~30%. Also, PYH5 and 6 kept the weight of zebrafish during the experiment (**Fig. 23 and 24**). The standards of liver damage with GOT and GPT were extremely increased by 1% EtOH treatment, whereas, PYH5 and 6 reduced the levels of GOT by 181.53 and 172.20 Karmen/ml, respectively in high dose group, and GPT was decreased to 140.87 and 277.0 Karmen/ml, respectively (**Table 2**).

3. 2. Liver inflammation inhibitory effectof PYH5 and 6 in ethanol damaged liver of adult zebrafish

The pro-inflammatory cytokines such as IL-1β, IL-6 and TNF-α were induced by treatment of 1% EtOH in zebrafish whereas high dose treatment of PYH5 and 6 reduced the pro-inflammatory cytokines (**Fig. 25**). Especially, PYH5 showed higher anti-inflammatory effects than PYE6 in EtOH damaged liver of adult zebrafish. However TGF-β1, mediator induced liver fibrosis, didn't get the affect from 1% EtOH for 3 weeks (**Fig. 26**).

3. 3. Liver cirrhosis model of adult zebrafish by CCl_4

CCl_4 treated group increased the death and weight loss of zebrafish (**not shown data**) and the standards of liver damage with GOT and GPT were extremely increased by 10% CCl_4 treatment (244.53 and 172.20 Karmen/ml, respectively) (**Table 3**). And the pro-inflammatory cytokines such as IL-1β, IL-6 and TNF-α were induced by treatment of 10% CCl_4 in zebrafish (**Fig. 27**). Especially, TGF-β1, mediator induced liver fibrosis, strongly got the affect from 1% EtOH for 3 weeks (**Fig. 28**).

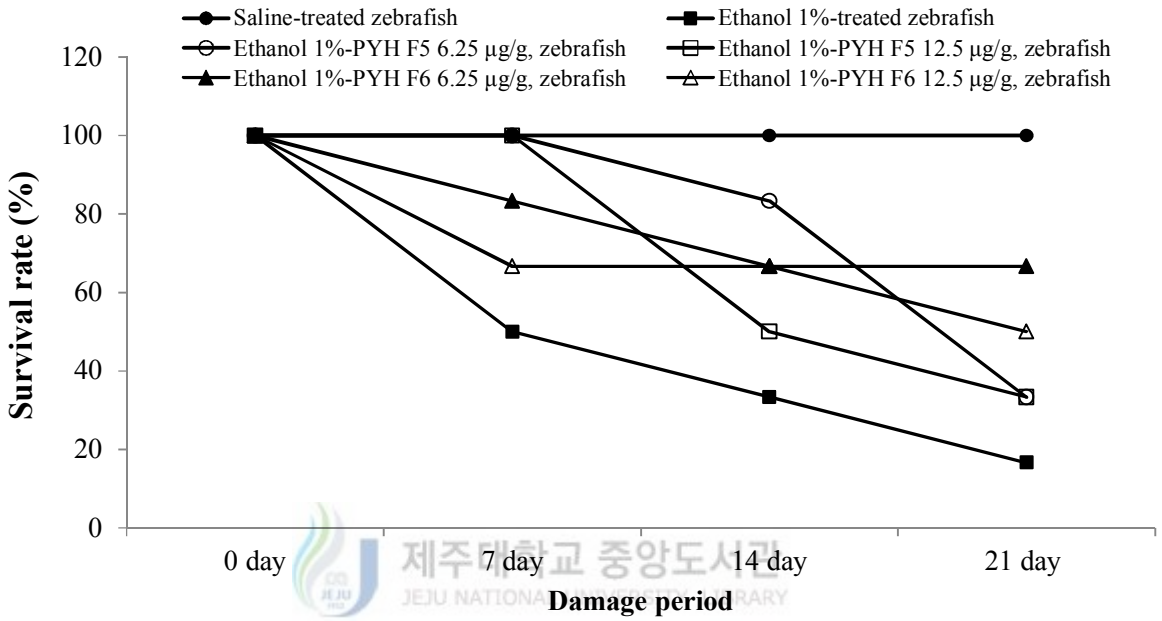

Fig. 26. Survival rate (%) of zebrafish damaged by 1% EtOH

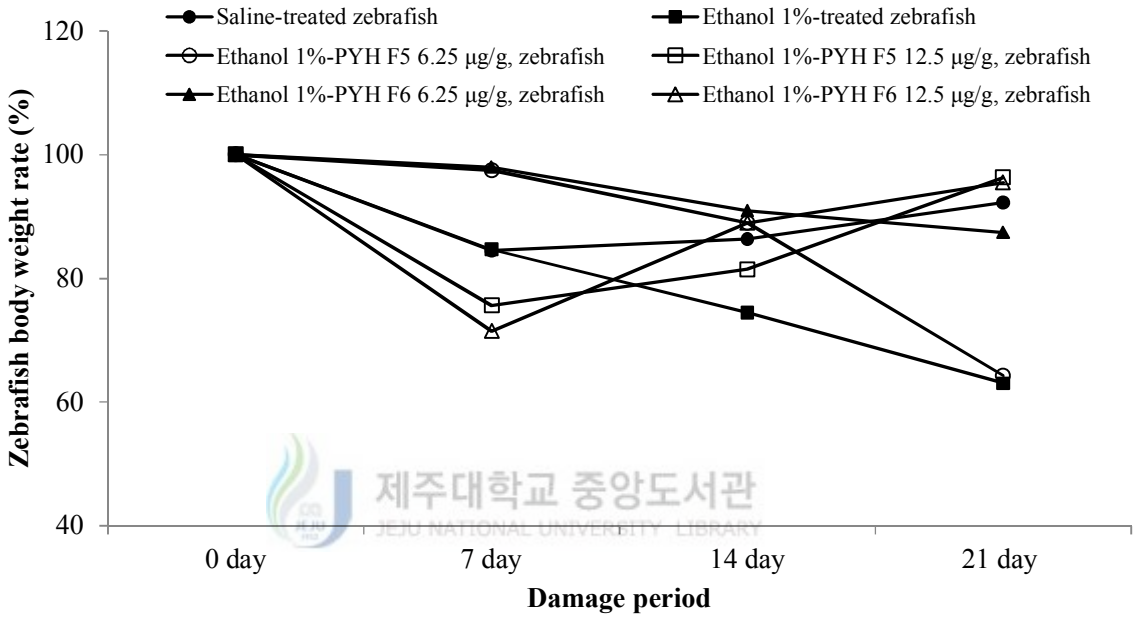

Fig. 27. Weight rate (%) of zebrafish damaged by 1% EtOH

Table.7. Liver damage of zebrafish by 1% EtOH

Groups	GOT (Karmen/ml)	GPT (Karmen/ml)
Saline-treated zebrafish	160.87±6.11	127.53±4.16
Ethanol 1%-treated zebrafish	240.87±7.57	297.40±7.01
Ethanol 1%-PYH 5 6.25 μg/g, Zebrafish	194.87±3.06	262.70±6.56
Ethanol 1%-PYH 5 12.5 μg/g, zebrafish	181.53±5.77	140.87±2.31
Ethanol 1%-PYH 6 6.25 μg/g, zebrafish	210.87±4.16	274.20±5.66
Ethanol 1%-PYH 6 12.5 μg/g, zebrafish	176.20±4.00	277.00±7.29

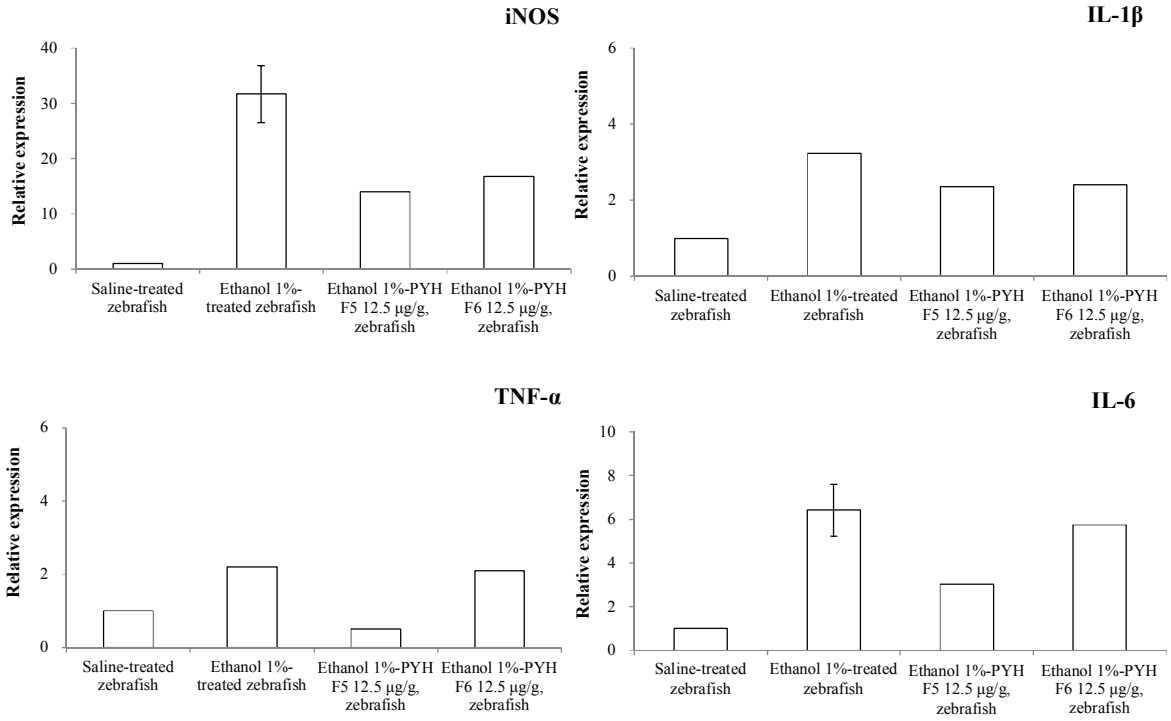

Fig. 28. Inhibitory effects of PYH5 and PYH6 against liver inflammation of zebrafish damaged by 1% EtOH

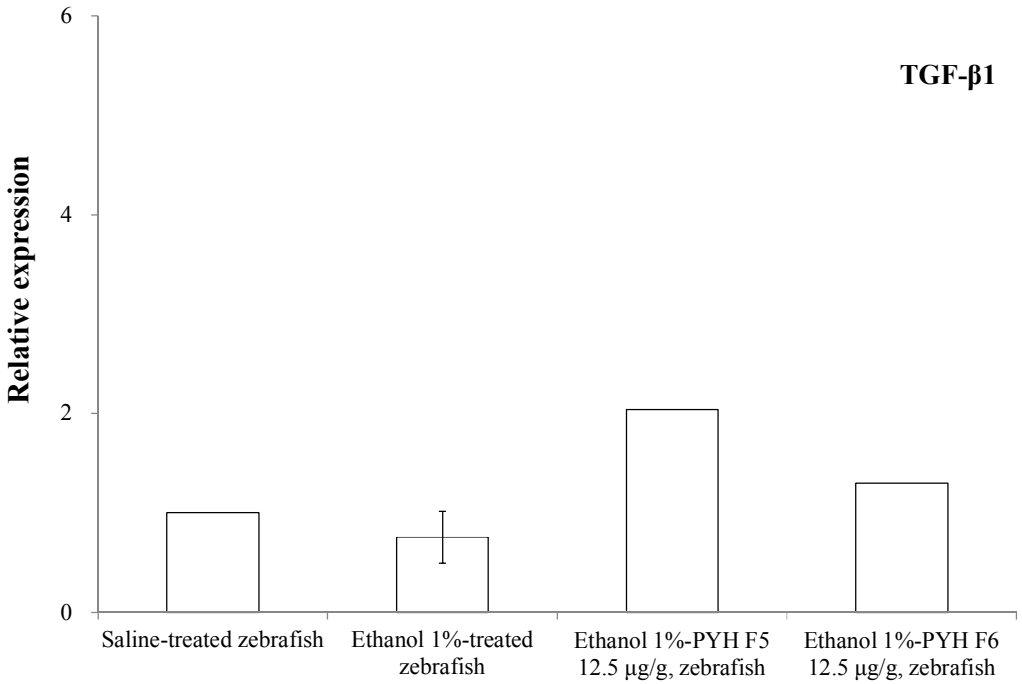

Fig. 29. Inhibitory effects of PYH5 and PYH6 against TGF-β1 induced by 1% EtOH in zebrafish

Table 8. Liver damage of zebrafish by 10% CCl_4

Groups	GOT (Karmen/ml)	GPT (Karmen/ml)
Soybean-treated zebrafish	188.87±4.16	196.20±5.66
CCl_4-treated zebrafish	244.53±7.31	274.60±7.92

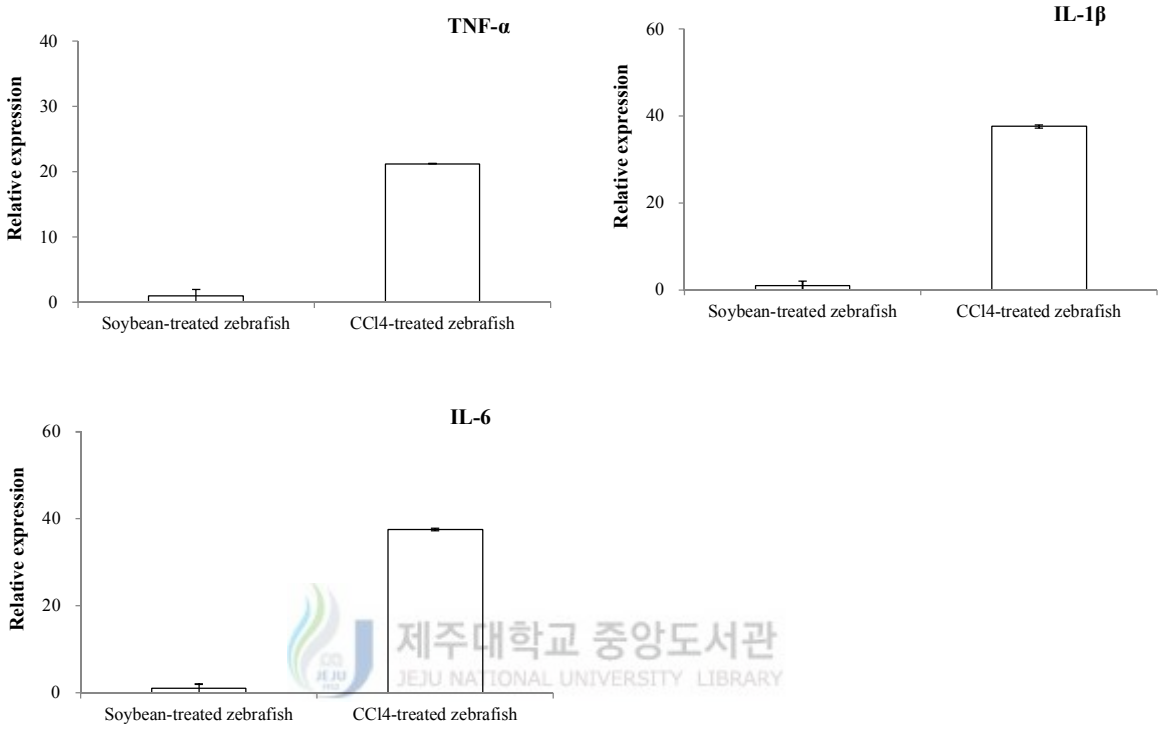

Fig. 30.liver inflammation of zebrafish induced by 10% CCl_4

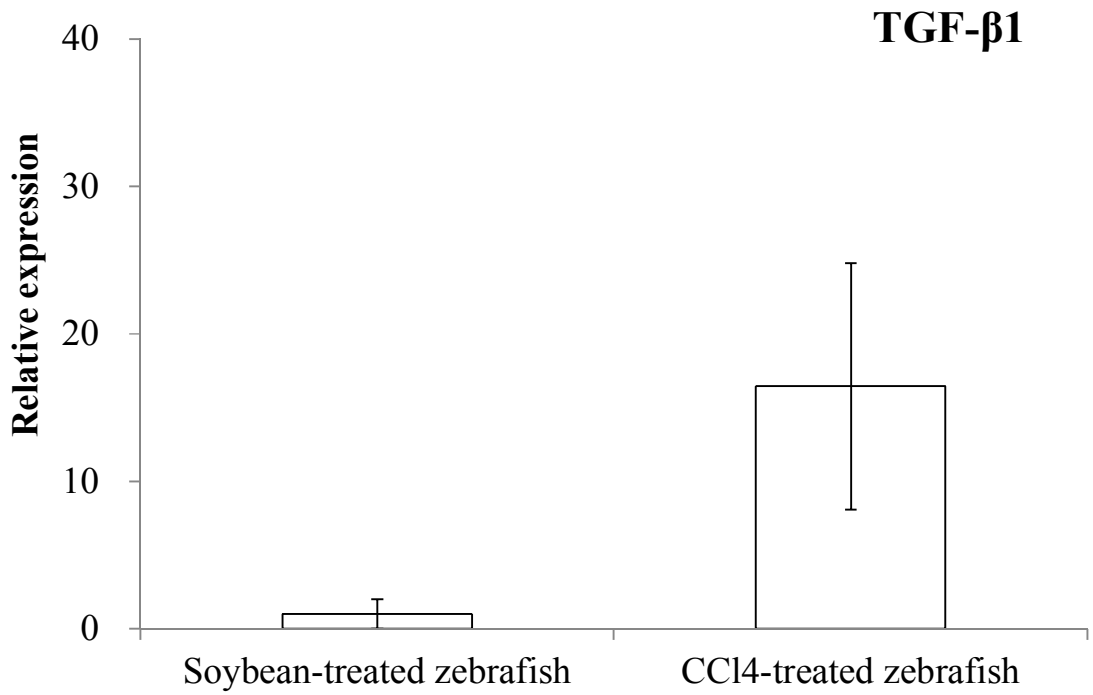

Fig. 31.TGF-β1 expression induced by 1% EtOH in zebrafish

Reference

1. K. Kazłowska, H. T. V. Lin, S. H. Chang,G. J. Tsai, Evidence-Based Complementray and Alternative Medicine, 2013, ID 493869: 10.

2. M. Senevirathne, C. B. Ahn, J. Y. Je, Food Science and Biotechnology, 2010, 19(6): 1551-1557.

3. Z. Zhang, F. Wang, X. Wang, X. Liu, Y. Hou, Q. Zhang, Carbohydrate Ploymers, 2010, 82(1): 118-121.

4. L. X. Zhang, C. E. Cai, T. T. Guo, J. W. Gu, H L. Xu, Y. Zhou, Y. Wang, C. C. Liu, P. M. He, Journal of Marine Science and Technology, 2011, 19(4): 377-382.

5. L. Qian, Y. Zhou, J. X. Ma, International Journal of Biological Macromolecules, 2014, 68: 48-49.

6. N. Inoue, N. Yamano, K. Sakata, K. Nagao, Y. Hama, T. Yanagita, Bioscience, Biotechnology, and Biochemistry, 2009, 73(2): 447-449.

7. C. S. Zhou & H. L. Ma, Food Science. 2006.

8. H. Qi, T. Zhao, Q. Zhang, Z. Zhao, R. Xing, Journal of Applied Phycology, 2005, 17: 527-534.

9. J. Wang, Q. Zhang, Z. Zhang, Z. Li, International Journal of Biological Macromolecules, 2010, 42(2): 127-132.

10. S. A. Mahesar, S. T. H. Sherazi, K. Abro, A. Kandhro, M. I. Bhanger, F. R. V. Voort, J. Sedman, Talanta, 2008, 75: 1240-1244.

11. J. Wang, J. Zhang, B. Zhao, X. Wang, Y. Wu, J. Yao, Carbohydrate Polymers, 2010, 80: 84-93.

12. X. Ye, L. Li, Anal, Chem, 2012, 84: 6181-6191.

13. A. O. A. C., Association of Official Analytical Chemists Washington, D. U.S.A., 1990

14. R. E. Cian, O. M. Augustin, S. R. Drago, Food Research International, 2012, 49: 364-372.

15. K. Takahashi, Y. Hirano, S. Araki, M. Hattori, Journal of agricultural and food chemistry, 2000, 48(7): 2721-2725.

16. M. Dubois, K. A. Gilles, J. K. Hamilton, P. A. Rebers, F. Smith, Anal. Chem, 1954, 28(3):

1783 350-356.
1784 17. K. Hiramoto, H. Johkoh, K. I. Sako, K. Kikugawa, Free radical research communications,
1785 1993, 19(5): 323-332.
1786 18. S. J. Heo, E. J. Park, K. W. Lee, Y. J. Jeon, Bioresource Technology, 2005, 96: 1613-1623.
1787 19. V. Gressler, N. S. Yokoya, M. T. Fuji, P. Colepicolo, J. M. Filho, R. P. Torres, E. Pinto,
1788 Food Chemistry, 2010, 120: 585-590.
1789 20. R. E. Cian, P. R. Salgado, S. R. Drago, R. J. Gonzalez, A. N. Mauri, Food Chemistry,
1790 2014, 146: 6-14.
1791 21. X. Yu, C. Zhou, H. Yang, X. Huang, H. Ma, X. Qin, J. Hu, Carbohydate Polymers, 2015,
1792 117: 650-656.
1793 22. B. N. Pramanik, U. A. Mirza, Y. H. Ing, Y. H. Liu, L. P. Bartner, P. C. Weber, A. K. Bose,
1794 Protein science, 2002, 11(11) 2676-2687.
1795 23. H. W. Vesper, L. Mi, A. Enada, G. L. Myers, Rapid Communications in Mass
1796 Spectrometry, 2005, 19(19): 2865-2870.
1797 24. Y. Chen, X. Gu, S. Q. Huang, J. Li, X. Wang, J. Tang, International Journal of Biological
1798 Macromolecules, 2010, 46: 429-435.
1799 25. R. M. Rodriguez-Jasso, S. I. Mussatto, L. Pastrana, C. N. Aguilar, J. A. Teixeira,
1800 Carbohydrate Polymers, 2011, 86: 1137-1144.
1801 26. S. Tsubaki, K. Oono, T. Ueda, A. Onda, K. Yanagisawa, T. Mitani,, J. I. Azuma,
1802 Bioresource Technology, 2013, 144: 67-73.
1803 27. K. Nomura, Y. Naitoh, S. Muramatsu, Y. Yoshizawa, J. Tsunehiro, F. Fukui, M. Itoh,
1804 Japan Society for Bioscience, Biotechnology, and Biochemistry, 1998, 62(6): 1190-1195.
1805 28. D. A. Navarro, M. L. Flores, C. A. Stortz, Carbohydrate Polymers, 2007, 69(4): 742-747.

29. Y. Hatada, Y. Ohta, K. Horikoshi, Journal of Agricultural and Food chemistry, 2006, 54(26): 9895-9900.

30. Z. Jiang, Y. Hama, K. Yamaguchi, T. Oda, The Journal of biochemistry, 2012, 151(1): 65-74.

31. K. Bock, C. Pedersen, Carbohydrate Research, 1985, 145(1): 135-140.